Journal of Hydrology (2006) **329**, 329–349

available at www.sciencedirect.com

ScienceDirect

journal homepage: www.elsevier.com/locate/jhydrol

Comparison of conventionally observed interception evaporation in a 100-m^2 subplot with that estimated in a 4-ha area of the same Bornean lowland tropical forest

Odair J. Manfroi [a,*], Koichiro Kuraji [a], Masakazu Suzuki [a], Nobuaki Tanaka [a], Tomonori Kume [a], Michiko Nakagawa [b], Tomo'omi Kumagai [c], Tohru Nakashizuka [d]

[a] *Graduate School of Agricultural and Life Sciences, University of Tokyo, 1-1-1 Yayoi, Bunkyo-KU, Tokyo-TO 113-8657, Japan*
[b] *Center for Ecological Research, Kyoto University, Kamitanakami-Hirano, Otsu, Shiga 520-2113, Japan*
[c] *Shiiba Research Forest, Kyushu University, Shiiba-son, Miyazaki 883-0402, Japan*
[d] *Research Institute for Humanity and Nature, Takashima-cho, Kamigyo-ku, Kyoto, 602-0878, Japan*

Received 21 February 2005; received in revised form 16 January 2006; accepted 17 February 2006

KEYWORDS
Water flow;
Interception evaporation;
Rainfall partition;
Throughfall;
Stemflow;
Tropical rainforests

Summary With the intention of determining mean annual interception evaporation (IE) or rainfall interception loss from a 4-ha area of lowland tropical forest in the Lambir Hills National Park, Sarawak, Malaysian Borneo, throughfall (TF) and stemflow (SF) were measured for 3-years within this area with both static SF and TF gauges located inside a 10×10 m subplot, called a fixed subplot, and relocation TF-gauges, i.e., TF-gauges that were moved periodically among 23 subplots (10×10 m) and in a transect line within the 4-ha plot area. The derived data showed that mean annual IE was 210 mm/year or 8.5% of the mean annual rainfall in the study period (2466.3 mm/year) in the 4-ha plot, and 295 mm/year or 12% in the fixed subplot. Both the 4-ha plot and the fixed subplot IE values were concluded to be reliable estimates and the 3.5% higher IE value observed in the fixed subplot likely due to a greater water holding capacity of the vegetation in the fixed subplot, where a large infrequent tree with thick bark but not projecting crown exists, than the mean condition in the 4-ha plot. Considering the derived data in the scale of 22 individual subplots where TF was measured for short periods with the relocation TF-gauges and in the fixed subplot, IE values from 3% to 25% in these subplots within the 4-ha area were thought sensible. This range of IE values within the 4-ha plot encompass the IE

* Corresponding author. Tel.: +81 3 5841 5214/5224; fax: +81 3 5841 5464.
E-mail address: manfroi@fr.a.u-tokyo.ac.jp (O.J. Manfroi).

0022-1694/$ - see front matter
doi:10.1016/j.jhydrol.2006.02.020

values claimed in most, if not all, previous rainfall interception case studies in natural lowland tropical forests.

Introduction

A fundamental part of land surface hydrology involves the quantification of rainfall partitioned into evaporation and runoff that much evidence suggest is affected by the cover type, specially by forest cover (Bruijnzeel, 1990; Calder, 1993; Brown et al., 2005). Biophysical process-based models at the global scale (e.g., Choudhury and DiGirolamo, 1998) or rainfall-runoff distribution models at the catchment scale (e.g., Calder, 2003) are examples of important tools in land use or water resources management that attempt to estimate evaporation and runoff from different cover types including forests. The output of these models may, for example, be compiled into evaporation maps or even web-based interactive evaporation and runoff maps, for which policy- or decision-makers can try out different land cover parameters and observe the changes in evaporation and runoff components (Calder, 2004). To develop, parameterize and validate such models, processes or field studies in the major land cover types of the world at different time and space scales are important. Specially useful for models testing, are information on the magnitudes of mean annual evaporation and runoff components, i.e., long-term representative areal mean annual values, and their inter-annual variation.

Land surface covered by tropical moist forest biomes is estimated to be approximately 12%, much of which is concentrated in three blocks in South America, central Africa and Southeast Asia (FAO, 1993; Whitmore, 1998). Although several water budget or processes studies have been conducted in these forests, long-term total evaporation and its partitioning into transpiration and interception evaporation (IE) are still debated. Mean annual IE values reported for many sites based on the conventional or wet canopy water budget method are specially variable, both among and within a same tropical moist forest formation sometimes not far apart. Because IE reviewers have often failed to explain the 5—45% range of mean annual IE values observed in case studies in these forests based on differences in the physical determinants know to influence IE such as site characteristics, forest type, and climate (Clarke, 1987; Shuttleworth, 1989; Crockford and Richardson, 2000; Kuraji and Tanaka, 2003), and also given the well documented high spatial variation, and problems of measuring throughfall (TF) and stemflow (SF) in forests (Jackson, 1971; Kimmins, 1973) the long back quotation by Horton (1919) is often remembered by IE investigators: the IE ''subject is one on which it is somewhat difficult to experiment in a satisfactory manner and many of the data are seemingly discordant''.

Quite satisfactory manners, i.e., instrumentation and methods, to study IE process at high time resolution have been developed. These would probably be the use of optical raingauges to observe precipitation (Habib et al., 2001), operation of eddy covariance systems during rainfall to measure true evaporation rates (Mizutani and Ikeda, 1994), net rainfall with plastic-sheet net-rainfall gauges (Calder and Rosier, 1976) or load-cell based troughs (Lundberg et al., 1997), and the use of remote sensing techniques to monitor time changes in the wetness degree and on the mass of water held in the whole forest (Calder and Wright, 1986; Bouten et al., 1996). The costs and skills required to operate such instruments are obviously prohibitive, specially in heterogeneous forests where several units would likely be required. As demonstrated in the long-term detailed study of Crockford and Richardson (1990c), however, the use of simple rainfall and TF gauges and measurements of SF, the case of the majority if not of all studies in natural tropical moist forests, and analysis at the rainstorm time scale should provide information on the effects of several forest and climate parameters on IE and accurate estimates of mean annual IE values as well as the magnitude of its inter-annual variation.

Changing the focus to lowland tropical forest formations, the relatively broad 5—22% range in mean annual IE values claimed in case studies in these forests (Bonell and Balek, 1993), sometimes in nearby sites, with the wet canopy waterbudget method is curious and usually difficult to explain with the documentation given in many studies on the site, observed plot, rainfall characteristics and the climate during the study or the factors explaining inter-storms or periods variation in IE. SF is also infrequently measured and a 1% value assumed. While recent studies in the Amazon basin reported mean annual IE values for somewhat similar lowland tropical forests from 5% to 13% (Leopoldo et al., 1995), in southeast Asia a same number of studies of similar accuracy have both reported values near 10% and near 20%. As in studies in southeast Asia, however, the values obtained in the studies in Amazon basin are also associated with high uncertainties, usually ±15%, except some studies in central Amazon where <5% error was claimed with relocation of TF-gauges technique, first proposed by Wilm (1943), and observation during a relatively longer period (Lloyd and Marques, 1988; Ubarana, 1996). As pointed out by Hölscher et al. (2004), relocation of TF-gauges might also yield uncertain values because the forest may change through time; moreover, by relocating TF-gauges it is difficult to study IE on the storm basis to understand governing factors causing variation in observed values. Thus, more observations, specially in southeast Asia lowland tropical forests, to improve understanding of IE, observation methods and its long-term magnitude are needed and important, specially if precipitation frequency, duration, intensity and magnitude are changing, as it appears the climate is, in the tropics (Malhi and Wright, 2004).

The objective of the present study was to compare the long-term about 3-years IE observed approximately daily in a small 100-m^2 subplot, called a fixed subplot, with that estimated in a 4-ha plot area of a natural Bornean lowland evergreen tropical forest, inside which the fixed subplot

was located. In addition, causes of TF and IE time and space variations in the 4-ha plot and fixed subplot are discussed in more detail.

Site

The study site is the crane 4-ha research plot, located in the surroundings of the large jib crane built in the Lambir Hills National Park, Sarawak, Malaysian Borneo (4°12′N, 114°02′E) for canopy processes studies. Fig. 1 shows the location and terrain around the study site in the Lambir Hills National Park located approximately 17 km from the South China Sea and 25 km south of Miri city. Most of the 70 km^2 of Lambir Hills National Park is covered by anthropogenic undisturbed lowland evergreen tropical forest. Inventorying all trees with diameter at breast height (DBH) > 1 cm in a 52 ha tract of this forest, Lee et al. (2002) characterized it as having emergent trees between 40 and 70 m height, a mean tree density of 6856 trees/ha with 91% of these trees between 1 and 10 cm in DBH, and a mean basal area of 43.3 m^2/ha. A total of 1173 species were identified in the 52 ha tract, with the most abundant species belonging to the Euphorbiaceae and Dipterocarpaceae families. Together, the dipterocarp species *Dryobalanops aromatica* and *Dipterocarpus globosus* contribute 13% of the total basal area. Overall, Dipterocarpaceae contribute 15.6% of the total number of trees and 41.6% of the total basal area. Euphorbiaceae species contribute 14.5% in terms of the number of trees, but just less than 6.6% of the total basal area. In the understory, trees of the species *Fordia splendidissima* of the Fabaceae family and the two Euphorbiaceae species *Croton oblongus* and *Macaranga brevipetiolata* are dominant in number.

Daily rainfall data measured between 1968 and 2001 at Miri Airport showed a mean annual rainfall of 2740.5 ± 378.98 mm. The mean number of rain days (>0.25 mm) in a year was 186, of which 114 days had rainfall of less than 10 mm. The mean annual temperature is 27 °C at Miri Airport. Above and within canopy micrometeorological observations in Lambir have started on January, 1999, first using only a scaffolding tree tower or the second tree tower (TTW2) of the canopy walkway system, used in ecological studies of the canopy, located about 500 m South of the crane, and from January, 2001 also using the crane in the 4 ha plot. Micrometeorological and hydrological results using these data as well more details on the present site can be found in related publications (Kumagai et al., 2001; Kumagai et al., 2004; Kumagai et al., 2005; Kuraji et al., 2001; Kume et al., 2005).

Vegetation characteristics in the 4-ha plot and in the fixed subplot

Fig. 2 shows the 4-ha plot surrounding the large jib crane gridded into 400 subplots of 10 × 10 m and the fixed subplot where we observed SF and TF continuously over the about 3-years duration of this study. The three dimensional and canopy projection map representation of 66 trees in the fixed subplot, drawn using allometric data described in Manfroi et al. (2004), shown in the left of Fig. 2 illustrates the high density of trees and interlocking of crowns in this forest. Table 1 summarizes some vegetation parameters derived in concurrent ecological studies or data we measured in this study in the 4-ha plot and in the fixed subplot. Canopy openness was calculated from 20 fish-eye lens photos taken in the fixed subplot and in other four subplots of the 4-ha plot, relative forest floor global radiation to above canopy radiation was also measured in these same subplots for short periods with self-made solar radiometers, and basal area (BA) or trees above ground biomass (TAGB) were estimated from DBH and tree height data and published allometric relationships between these parameters and biomass of

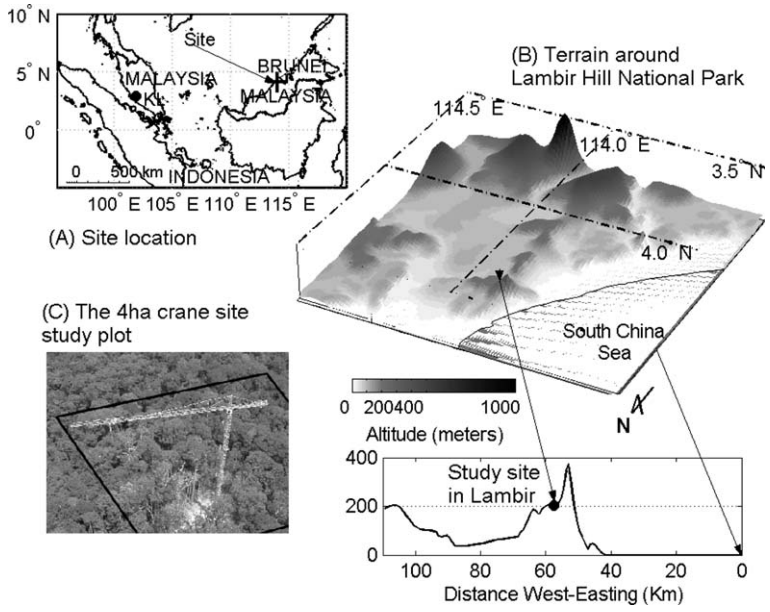

Figure 1 Site location and terrain around Lambir Hills National Park (elevation data from DTED Level 0 (NIMA, 1996) displayed with 20-fold vertical exaggeration).

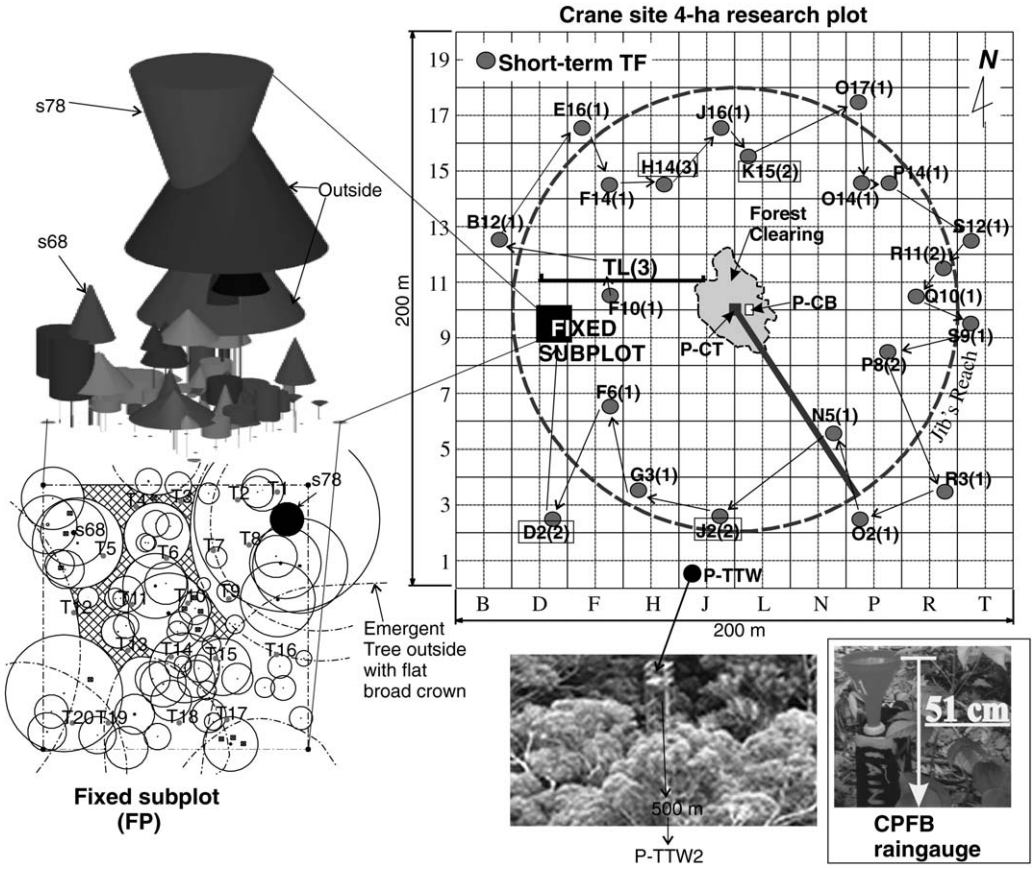

Figure 2 Layout of measurement in the 4-ha plot. Showed are the location of gross rainfall measurements (P-CT, P-CB, P-TTW, and P-TTW2); the fixed subplot, the subplots and the transect line where short-term TF observations where carried out in the first two years of this study and in the latter 3 months of the third year (subplots with names inside rectangles) with the relocation TF-gauges, see text. (*Note*: The number of times TF was observed in a given subplot or transect line is indicated aside the subplot's name, e.g., TL(3) means short-term TF measurements were taken 3 times in the transect line over the 3-years. The arrows from subplot to subplot illustrates the migration of the relocation TF-gauges in the first 2-years.)

Table 1 Comparison of vegetation characteristics in the 4-ha plot with the fixed subplot

	4-ha plot		Fixed subplot	
	Mean	Range	Mean	Range
Leaf area index (m^2/m^2)[a]	6.2	4.8–6.8	–	–
Canopy openness (%)	6.4	3–9	5.1	4–6
Relative forest floor radiation (%)	9.7	3–15	8.8	7.0–11.4
Trees/ha[b]	6442	–	6600	–
BA (m^2/ha)[b]	41.8	–	145.0	–
TAGB (t/ha)[b]	494.1	–	2311.0	–
Stemless palms/subplot	–	0–5	0	–

[a] Kumagai et al. (2005).
[b] Data for trees <10 cm measured in only 23 subplots.

trees (Chave et al., 2003). The vegetation in the 4-ha plot and in the fixed subplot are similar in terms of canopy openness, and perhaps leaf area index, or tree density but differ greatly in terms of basal area or TAGB due to an infrequent large tree in the fixed subplot (s78, Fig. 2). This is also suggested in Fig. 3 which shows the spatial variation of TAGB per subplot of the 4-ha plot. Subplots such as the fixed subplot with TAGB > 15 t (1500 t/ha) are only six in the 4-ha plot due to a large tree that usually has a broad, often >150 m^2, emergent crown and large buttresses. The large tree in the fixed subplot or tree s78 although with a thick bark and buttressed trunk have a small crown (39 m^2) not projecting far from the main canopy layer and with substantially fewer leaves. Also, in many subplots of the 4-ha plot

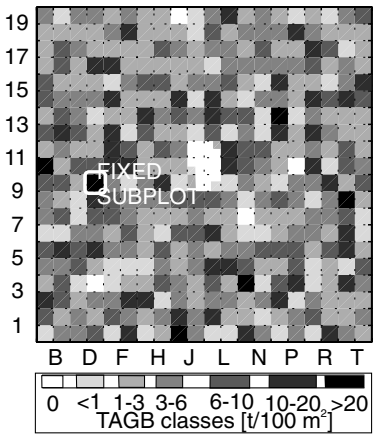

Figure 3 Spatial variation of estimated total above-ground biomass of trees (TAGB), using allometric relationships, per 10 m × 10 m subplot of the 4-ha plot.

1—5 stemless palm trees may occur, but none is found in the fixed subplot. In lowland tropical forests of southeast Asia and south or central America TAGB varies between 200 and 650 t/ha, being the largest values claimed in southeast Asia (Chave et al., 2003); spatially, TAGB is highly variable within a same lowland tropical forest. Numerous palms, lianas and understory trees are also often found in these forests.

Measurements

Gross rainfall

The raingauge devices used in this study were standard 200 mm tipping buckets (RS102, Ogasawara Keiki, Tokyo, Japan) and self-made manual raingauges or combination of plastic funnel and bottle raingauges (CPFB). The nominal depth of the bucket of the tipping buckets was 0.5 mm and its tip timing (date and time at 0.5-s resolution) was recorded with HOBO event data-loggers (Onset Instruments). The CPFB manual raingauges, used also in the TF measurements, consisted of a steep plastic funnel (∅ = 206 mm) assembled in black colored 10 L capacity plastic bottles (a photo of this raingauge is shown in the bellow right corner of Fig. 2). The water that accumulated in the CPFB manual raingauges was recorded by emptying the bottles into 1 L plastic cylinders with 10 mL graduations. Evaporation loss from these manual raingauges was not estimated but based on previous studies (Lloyd and Marques, 1988), were perhaps much smaller than the human errors likely for readings of the 10 mL or 0.3 mm graduated cylinders. Also, to empty the CPFB raingauges at ground level the funnels had to be detached in every measurement and leveled to the horizontal.

Rainfall in the 4-ha plot was monitored at ground level in the about 600 m^2 forest clearing made to build the crane's basement with two CPFB raingauges and one standard tipping bucket (STB) raingauge; above canopy in the crane top, 85.8 m above ground level, with a STB raingauge, and in the top of a tree tower supported in an emergent tree about 53 m above the forest floor and 10 m apart from the main canopy layer with two CPFB raingauges (Fig. 2). A 55 m long plastic hose (∅ = 20 mm) connected the funnels of the CPFB raingauges in the tree tower top to the bottles in the forest floor to allow for daily readings. Testing just after installation indicated that <0.18 mm (3—6 mL) were lost to wet this hose. In fact, one of the funnels (∅ = 200 mm) used in the tree tower top was a standard storage raingauge made of metal and with cylindrical shape. In addition to these rainfall measurements in the 4-ha plot with six raingauges, rainfall observation with a STB raingauge has also been in operation in the top of TTW2 since January, 1999 (Fig. 2).

Static long-term SF and TF measurements in the fixed subplot

For the whole study period of about 3-years, static TF and SF gauges were operated in the fixed subplot, i.e., the TF-gauges remained in the same position and the SF collar type gauges attached on the same trees. Analysis of the SF produced by individual trees and the SF generation dependence on trees's size parameters as well as the SF collar type gauge description was reported in Manfroi et al. (2004) using data collected from 1 July 2001 to 30 June 2002 or the first year of this study. In summary, SF collar type gauges were attached to the boles of 78 trees with a DBH > 1 cm and height > 1 m in the fixed subplot; also, three trees of intermediate size, not occurring in the fixed subplot, were observed outside the fixed subplot. The static TF observation in this subplot were made with 20 CPFB raingauges, hereafter fixed TF-gauges, placed in five lines crossing the fixed subplot area. The positions of the fixed TF-gauges (T1—T20) are indicated in the crown projection map in the left bellow corner of Fig. 2. Using the same procedure in the manual rainfall measurements, SF volumes accumulated in 30 L bottles and TF in the fixed TF-gauges were recorded daily; SF volumes of 10 high SF yielder trees, however, were recorded with tipping buckets.

Migrating short-term TF measurements in the 4-ha plot and fixed subplot

The spatial variability of TF in the 4-ha plot and fixed subplot was assessed from short-term TF measurements using additional TF-gauges, referred to as relocation TF-gauges, varying from 20 CPFB raingauges during the first 2-years (2001/07—2003/07), 40 CPFB raingauges in the first 6 months of the third study year (2003/07—2004/01) and 80 CPFB raingauges in the latter 3 months of this study (2004/04—2004/07).

The positions in the 4-ha plot where short-term TF was observed with the 20 relocation TF-gauges in the first 2-years are shown in Fig. 2. Basically, after more than 10 daily measurements were observed in a given position the relocation TF-gauges were migrated to a new subplot or a transect line. The time the relocation TF-gauges remained in a same position varied from 14 to 47 days with a mean of 26 days or about a month depending on the frequency of rainstorms. Overall, in these 2-years, the relocation TF-gauges were migrated 29 times including 1 time in the fixed subplot; 2 times in subplots H14, P8 and R11; 3 times in the transect line; and

1 time in each of 19 other subplots (Fig. 2). Therefore, in the first 2-years, 40 TF-gauges were operated, the 20 fixed TF-gauges in the fixed subplot and the 20 relocation TF-gauges migrated periodically among 23 subplots, including the fixed subplot, and a transect line.

In the first 6 months of the third study year, the number of relocation TF-gauges was doubled and added to the fixed TF-gauges in the fixed subplot. Thus, in this period TF in the fixed subplot was observed with 60 TF-gauges, i.e., the 20 fixed TF-gauges and 40 relocation TF-gauges. The intent of this observation was to understand the TF spatial variability in this subplot, and the representativeness of the points observed with the fixed TF-gauges in the 3-years. In the 3 months period that followed this intense measurement in the fixed subplot, due to unforseen problems, only the fixed TF-gauges were operated. Finally, in the latter 3 months the number of relocation TF-gauges was increased to 80 CPFB raingauges, and distributed in two pairs of subplots, H14&K15 and D2&J2, separated by 120 m, see Fig. 2, and where in the first 2-years a relatively high TF was observed. The purpose of this more long lasting observation was both to check the more short-term observations done during the first 2-years, and determine if during the 3 months differences in TF among these subplots could have been due to differences in incident rainfall in these two positions 120 m apart. Therefore, in the latter 3 months of this study 100 TF-gauges were operated in the 4-ha plot, the 20 fixed TF-gauges in the fixed subplot and 20 relocation TF-gauges in each of four subplots.

Continuous and single storm data sets

Every weekday and on Saturdays around 8 AM (LST) in the study period the crane or 4-ha plot site was visited by the same research assistant trained to carry out the manual measurements, or by ourselves. If after checking the manual raingauges some rainwater was found inside the bottles, then SF and TF measurements were carried out, otherwise rainfall, SF and TF were assumed to be zero in that day. Thus, TF or SF that could have originated inside the forest from other rainfall sources such as fog or condensation in the forest leaves were assumed to be negligible. Integrating this approximately daily time series to intervals within which one or more rainfall events occurred, i.e., $P > 0$, and complete data for all manual raingauges, manual SF-gauges, fixed and relocation TF-gauges operated in the period were collected for the corresponding rainfall, a 368 irregularly spaced time series data set resulted. A column marking the location of the relocation TF-gauges in the 4-ha plot in each of these irregular periods was added to this data set. Rainfall and SF recorded automatically with tipping buckets were summed up to match the irregular time intervals and added to this continuous manually recorded about 3-years data set.

Using the tip timing of the bucket of the crane top tipping bucket and assuming a dry spell greater than 6 h between the cessation of one storm and the start of the next, or inter-arrival time >6 h, the time intervals with only one such storm were noticed in the 368 irregularly spaced continuous 3-years data set. The number of measured singled storm intervals were 148 in the 3-years; most intervals contained two storms, as it will be shown latter this was because daily readings were only made in the morning between 8 AM and 2 PM but rainfall events occur frequently both around noon and in night time in Lambir. For each of the 148 single storm measurements as well as for all the single events occurred in the 3-years ($n = 662$), 19 rainfall and during rainfall meteorological conditions related parameters were calculated using data from the crane top tipping bucket and the 10-min meteorological time series usually measured at the crane's fourth stage, about 75.5 m above the ground level (Kumagai et al., 2004). The rainfall parameters needing definition for later analysis, are the first and last tip time of the bucket in the event and by difference the event duration (D), the mean rainfall intensity ($\overline{I_P}$), and a measure of within rainfall event intensity spike or maximum 10-min intensity ($IMAX_P$). Based on the work of Habib et al. (2001), these parameters are sufficiently accurate determined from 0.5 mm tipping bucket data. Meteorological parameters mentioned later are mean air vapor pressure deficit ($\overline{VPD}$), mean wind speed ($\bar{u}$), mean air temperature ($\overline{T}$), and mean wind direction or predominant wind direction. All these meteorological parameters were calculated by averaging the 10-min time series meteorological data between the first and the last tip of the bucket in the storm.

Method for estimating IE in the fixed subplot and 4-ha plot

Interception evaporation (IE) was computed as the difference between rainfall and net rainfall or $IE = P - (TF + SF)$. In the fixed subplot, because of continuous recording, in any period the TF associated with a given accumulated rainfall (P) is the arithmetic accumulated mean catches by the 20 fixed TF-gauges, and SF is the total volume yield by all trees in this subplot in the period transformed to depth or millimeters by using the subplot area or 100 m^2. To consider IE in the 4-ha plot or in the individual relocation subplots, where only short-term TF measurements were carried out, at yearly or longer time scales, both TF and SF were extrapolated or scaled up. For TF this was done by deriving empirical linear models of the form $TF = -b + a \cdot P$, where a and b are empirical coefficients determined by least squares fitting on TF against P data collected in the short-term TF measurements in the relocation positions. These equations were then applied to the rainfall depth in storms occurring in a considered period outside the short-term TF measurements in a relocation position. If the storm's rainfall depth was $<b/a$, the amount of rainfall needed for TF commencement; however, zero TF was assumed in the storm. The 4-ha plot TF is then assumed equal the arithmetic mean of TF ''observed-estimated'' in all relocation positions and observed in the fixed subplot in the considered period. SF in the 22 individual relocation subplots was scaled up by applying the results of 69 measured individual trees in the form of stemflow volume ratio [SVR = SF(mL)/P(mm)] to DBH linear relationships to DBH > 1 cm data, collected for the trees in these subplots, and rainfall amount in a considered period. The 4-ha plot SF is then assumed equal the arithmetic mean of estimated SF in the 22 relocation subplots and observed in the fixed subplot in a considered period.

Results and discussion

Rainfall measurements accuracy and reference rainfall

Table 2 shows total rainfall caught by the six raingauges in the 4-ha plot and one raingauge on the top of second tree tower (TTW2) in the years 2002 and 2003 when complete record was available for these gauges. Among these raingauges, only those installed on the tree tower top in the 4-ha plot (TTW_1 and TTW_2) were at same level and just 0.5 m from each other. Comparing different devices, i.e., STB and CPFB raingauges, it can be seen that in the 2-years STB raingauges underestimated the CPFB raingauges by about 155 mm. On the other hand, comparing differences among a same device in the forest clearing and above canopy a 205 mm overestimation favoring ground level raingauges occurred in the 2-years. In addition, while the 2-years difference among the STB raingauges at CT and TTW2, 500 m apart, was negligible, on an annual basis it was 4.3% in year 2003, and on a monthly basis the total amounts caught between these two raingauges varied by ±10%.

Fig. 4A–C shows the differences in catches among the 4 CPFB raingauges in single storms. As shown in Fig. 4A and B the differences in catches by the two co-located CPFB raingauges on the tree tower top or in the crane base was <5% and tended to increase with *P* in the storm, but patterns for specific wind directions are not evident. On the other hand, the differences between the mean catches of the two CPFB raingauges in the crane base and those on the tree tower top was relatively more scattered, and patterns for specific wind directions are somewhat evident (Fig. 4C); i.e, if wind was predominantly from East directions in a storm the crane base raingauges tended to catch greater rainfall and if it was from West directions their catches tended to be less than the catches by the tree tower top raingauges. Blow-in or splash of rain droplets into the crane base raingauges, rain shadows created both by the crane structure and nearby trees over the crane base raingauges in storms with angled rain, and aerodynamic loss of rain droplets blown across the top of the catching orifice of the tree tower top raingauges exposed to wind are causes that could have created such patterns and the higher scatter in

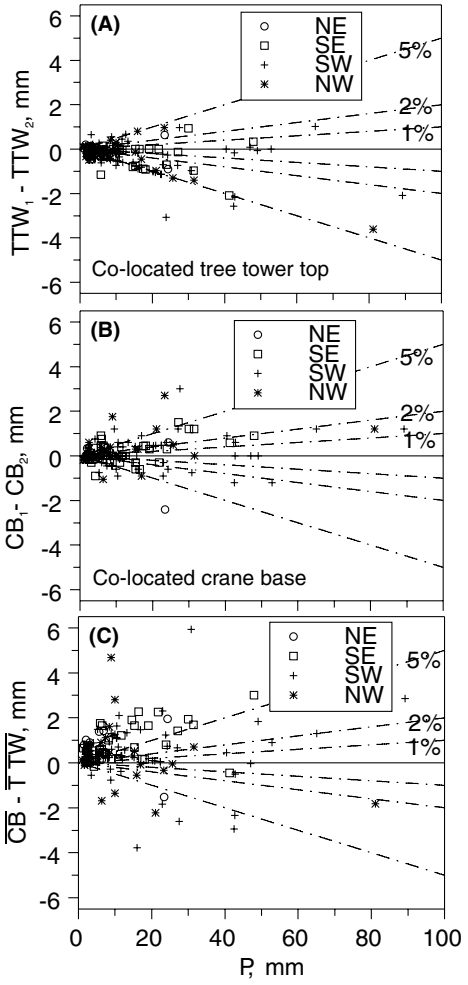

Figure 4 Relationship of catch differences between the 4 CPFB raingauges in the 4-ha plot with average total rainfall caught by these raingauges in single storm measurements. (*Note*: The style of the symbols varies with the predominant wind direction, see text.)

Fig. 4C than for co-located raingauges. Usually, wind is gentle in the present site (<5 m/s) and rainfall of high intensity, under these conditions aerodynamic losses are unlikely to be significant (Crockford and Johnson, 1983); moreover, clear

Table 2 Accumulated rainfall recorded with standard tipping buckets (STB) and with manual CPFB raingauges between January 2002 and December 2003

	STB			CPFB			
	CT	CB	TTW2	CB_1	CB_2	TTW_1	TTW_2
Installation height (m)	85.8	1.5	50	0.51	2	53	53
Distance from crane's center (m) (direction)	5	5(E)	500(S)	5(E)	6(E)	100(S)	100.5(S)
Diameter (cm)	20.0	20.0	20.0	20.6	20.6	20.6	20.0
Accumulated *P* (mm)							
2002	2191.0	2270.0	2118.0	2355.5	2331.0	2312.7	2253.8
2003	2262.5	2400.0	2362.5	2488.4	2482.5	2338.4	2338.5
2002–03	4453.5	4670.0	4480.5	4843.9	4813.5	4651.1	4592.3

CT: crane top, CB: crane base, TTW: tree tower top, TTW2: second tree tower.

patterns of highly different catches by above canopy raingauges in relation to ground level or between co-located raingauges under strong wind (>3 m/s) and light rainfall intensity (<5 mm/h) were not evidenced by graphical analysis.

Many interception studies pay little attention to gross precipitation measurement (Crockford and Richardson, 2000), some do not even state adequately the position of raingauges; however, sufficient accurate precipitation values for IE calculation are difficult to achieve, specially at the storm time scale. This was the case in our 4-ha plot where only narrow inadequate clearing is available for precipitation observation at ground level, and observations at quite short distance apart from the 4-ha plot would be unrepresentative due to the large spatial variation signature of tropical rainfall. Above canopy observations might also have been prone to wind caused under-catches in many events. The differences in catches by co-located CPFB raingauges on the tree tower top, shown in Fig. 4A, would suggest errors on daily readings of ±5% perhaps caused by human factors, but most likely due to no obvious causes, as also concluded in other studies (Crockford et al., 1996). This variations among co-located raingauges catches; however, are comparable to some previous studies where differences ranged from 1% to 8% (Marin et al., 2000; Dykes, 1997; Chappell et al., 2001). Considering the 4 CPFB raingauges in the 4-ha plot, the difference between the maximum catch and minimum catch among these raingauges in the 148 single storms data set differed quite often by more than 2 mm (Fig. 4) and for seven events the difference was >4 mm. This are very large differences compared with some other studies where differences >0.5 mm were rare (Rutter, 1963) or no significant difference among storm total catches for exposed and not exposed to wind raingauges were found (Lloyd and Marques, 1988). Unlikely in studies where a wide and adequate clearing was available to measure gross rainfall (Crockford et al., 1996; Crockford and Richardson, 1990a; Crockford and Johnson, 1983), analysis of wind direction and wind speed in the present study did not help to select the gauges with correct catches. Therefore, reference rainfall for IE calculation was assumed equal the arithmetic mean amount caught by the 4 CPFB raingauges if their catches were consistent, if one or two of the raingauges appeared to have strange observed values, including also the two STBs raingauges' catches in the comparison, these strange values were treated as missing values. As it will be discussed later, however, in storms when a negative IE resulted for observations in the fixed subplot the maximum catch among the six raingauges in the 4-ha plot was used.

Synoptic of rainfall and climate during storms in the study period

Table 3 shows yearly accumulated average rainfall caught by the CPFB raingauges and by STBs. In all yearly studies annual rainfall was bellow the climatological annual mean of about 2740 mm. The close agreement between accumulated amounts caught by the STB in the top of TTW2, the STB in the crane base and the average of the 4 CPFB raingauges in the latter study year (Year 3) shown in this table, gives more certainty for the P records in this year. In the study period there were 662 rainfall events being the most numerous storms with $P < 10$ mm (Table 4). The contribution of these storms of small magnitude to total rainfall in the study years was <21%; in addition, though in the first study year storms of small size were relatively more frequent, the contribution to total annual rainfall from storms in different size classes were constant among the years, and mostly attributable to storms with $P > 20$ mm. Analysis of 10-min accumulated rainfall caught by the STB in the crane top suggested for the 662 rainfall events a mean intensity of 9.8 mm/h; on the other hand, analysis of hourly accumulated totals, excluding single tips and hours with $\leqslant$0.5 mm, suggested a 5 mm/h mean rainfall intensity over

Table 3 Accumulated average rainfall caught by the 4 CPFB raingauges and by STBs raingauges in the study period

	Accumulated P (mm)			
	Year 1	Year 2	Year 3	Years 1–3
CPFB (ground and above)	2292.0	2439.0	2668.0	7399.0
STB CB (ground)	2234.0	2304.5	2635.5	7174.0
STB CT (above)	2150.5	2206.0	2507.5	6864.0
STB TW2 (above)	2092.5	2201.0	2641.0	6934.5

Year 1: 01 July 2001–30 June 2002; Year 2: 01 July 2002–30 June 2003; and Year 3: 01 July 2003–17 July 2004.

Table 4 Number and contribution of rainfall events (inter-arrival time = 6 h) to total rainfall

	Year 1	Year 2	Year 3	Years 1–3
Total, n (% of total P)	226(100)	211(100)	225(100)	662(100)
P classes (mm), n (% of total P)				
<10	168(21)	146(21)	149(21)	463(21)
>10	58(79)	65(79)	76(79)	199(79)
>20	33(61)	35(60)	40(58)	108(60)
>40	11(34)	14(34)	11(26)	36(31)

Table 5 Average of rainfall and meteorological parameters of storms in each yearly period

	Events/day	$\overline{P}$ (mm)	$\overline{D}$ (h)	$\overline{I_P}$ (mm/h)	$\overline{IMAX_P}$ (mm/h)	$\overline{VPD}$ (kPa)	$\bar{u}$ (m/s)
Year 1	0.62	9.5	2.95	3.2	20.6	0.29	2.17
Year 2	0.58	10.4	3.04	3.4	22.1	0.19	2.05
Year 3	0.59	11.1	3.08	3.6	24.5	0.20	2.16

the 3-years. The mean duration of the 662 storms in the 3-years was 3 h. Table 5 shows the average of some rainfall and meteorological related parameters, defined in 'Continuous and single storm data sets' section, per yearly study. As shown, relatively more storms of lower intensity, but associated with higher air vapor pressure deficit and stronger wind happened in Year 1 than in Years 2 and 3.

Fig. 5 provides a description of rainfall in the study period using hourly and monthly accumulated amounts. As shown, monthly rainfall was somewhat evenly distributed, but remarkably less rainfall occurred in February 2003 and February 2004. Both rainfall and climate in this region are influenced by the southwest Monsoon, usually from late May to September, and the northeast Monsoon, from November to March. Also, during the study period there was an warm phase of the El Niño Southern Oscillation (ENSO), left of Fig. 5, that could be related to the somewhat different rainfall in the second half of Year 2 and beginning of Year 3. As apparent in Fig. 5, rainfall in the present site is composed of relatively more intense storms occurring between 1 and 4 PM, and less intense longer duration storms between 9 PM and 6 AM. In fact, in the 3-years more than 50% of the total rainfall was due to events that started and ended between 4 PM of a given day and 10 AM of the next day. During these night and morning time events, rainfall intensity, vapor pressure deficit and wind speed were considerably lower than during the events that happened in the afternoon; on the other hand, while mean duration of afternoon events was only 1 h, that of night time events was 4.5 h. Comparatively, in central Amazon and Pasoh forest reserve, Peninsular Malaysia, rainstorms are more likely to occur in the afternoon and late afternoon and only small amounts in the morning time (Lloyd, 1990; Oki and Musiake, 1994; Noguchi et al., 2003).

Partitioning of rainfall in the fixed subplot at the storm and yearly time scales

Fig. 6 shows scatterplots between the fractions of rainfall partitioned into TF, SF and IE in the fixed subplot against

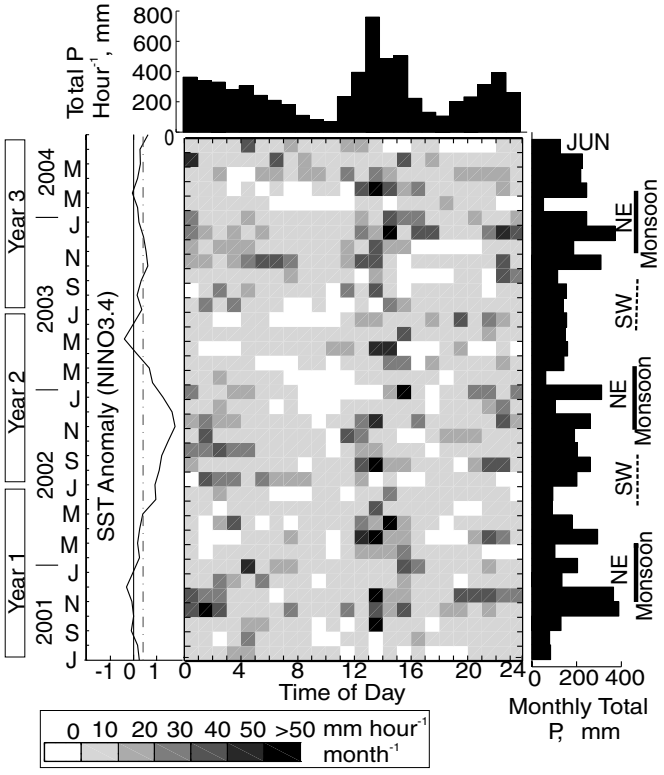

Figure 5 Synoptic of rainfall in the study period. Middle panel grid illustrates the diurnal rainfall occurrence pattern or total rainfall per a given hour per month, monthly rainfall are shown in the right panel, and total rainfall observed in a give hour of a day over the 3-years in the upper panel. Also, in the right panel monthly values of sea surface temperature (SST) index at NINO3.4 region is shown.

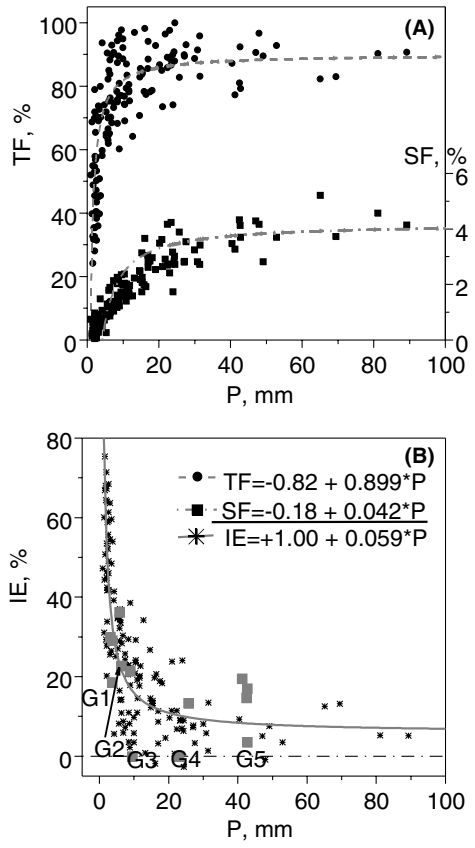

Figure 6 Partitioning of total rainfall into TF, SF and IE in the 148 single storm measurements data set observed in the fixed subplot over the 3-years study.

accumulated rainfall in each of the 148 single storm measurements data set. As shown, in storms with $P < 10$ mm both TF and SF tended to be considerably lower; moreover, high TF fractions were observed after only 5 mm of rainfall, but >20 mm amounts were needed to maximize SF. For all ranges of rainfall amounts observed in these events IE was very variable, and five events with negative interception values resulted even after the use of the maximum rainfall caught among the six raingauges in the event. Because of the large coefficients of variation (mean = 30%, range = 16–63%), among the 20 fixed TF-gauges catches in these storms, uncertainties in rainfall measurements, and the high non-linear nature of IE inter-storms variation (Llorens et al., 1997), it is difficult to confidently determine the most relevant factors causing the high scatter in Fig. 6. Nevertheless, some likely important rainfall and meteorological factors are suggested for some selected events (Crockford and Richardson (2000) analysis), and by stepwise and multiple linear regression analysis. In the scatterplot of IE against P in Fig. 6 five groups of events (G1–G5) of increasing depth are marked. Table 6 shows some rainfall and meteorological parameters for each event in these groups. As can be concluded from a consideration of the data in this table, the highest IE amounts in a group were observed for events of a long duration, low intensity and with small intensity spikes or peaks (low $IMAX_P$) during its occurrence, and associated with high vapor pressure deficit or strong wind. Similar conclusions are suggested by the multi-linear regression model showed in the last line of Table 6. This model was computed by selecting among 19 standardized variables (mean = 0, SD = 1) related to rainfall intensity and meteorological conditions during 96 storms, extracted from the single storm measurements data set, with magnitude between 1.5 and

Table 6 Rainfall and meteorological parameters for the groups of storms noted in Fig. 6

	Start	End	P (mm)	IE (mm)	IE (%)	D (h)	$\overline{I_P}$ (mm/h)	$IMAX_P$ (mm/h)	$\overline{VPD}$ (kPa)	$\bar{u}$ (m/s)
G1	12/27/02 23:01	12/28/02 02:21	3.7	0.7	18.5	3.3	1.1	3.0	0.0	1.3
G1	05/23/02 21:35	05/24/02 02:51	3.1	0.9	29.9	**5.3**	**0.6**	3.0	0.0	**1.4**
G1	08/18/03 18:30	08/18/03 21:50	3.7	1.1	29.1	3.3	1.1	3.0	0.0	1.2
G2	08/27/03 13:21	08/27/03 14:08	6.4	1.4	22.7	0.8	8.1	12.0	**0.4**	1.9
G2	04/15/03 11:46	04/15/03 13:06	5.8	2.1	36.2	**1.3**	**4.4**	**6.0**	0.2	**2.4**
G3[a]	07/18/03 22:32	07/18/03 23:47	9.5	0.0	−0.1	1.2	7.6	27.0	0.0	2.8
G3	09/03/03 01:10	09/03/03 09:40	8.9	1.9	21.4	**8.5**	**1.1**	**3.0**	0.0	1.9
G4	10/01/03 12:01	10/01/03 12:34	23.0	0.0	−0.1	0.6	41.0	72.0	0.1	2.0
G4	10/26/01 13:27	10/26/01 14:31	25.7	3.4	13.3	**1.1**	**24.2**	102.0	**0.5**	**4.4**
G5	10/02/01 21:58	10/03/01 09:42	42.8	7.3	17.0	**11.7**	**3.6**	60.0	0.0	1.3
G5	11/18/01 20:46	11/19/01 03:41	41.2	8.0	19.5	**6.9**	6.0	**30.0**	0.0	**2.1**
G5	04/15/02 02:29	04/15/02 08:07	42.5	6.2	14.6	5.6	7.5	54.0	**0.1**	1.4
G5	01/14/03 17:59	01/15/03 01:39	42.7	1.5	3.5	7.7	5.6	48.0	0.0	1.5

MLeq $IE_{STZ} = -0.2 \cdot \overline{I_P} - 0.4 \cdot IMAX_P + 0.4 \cdot \overline{VPD} + 0.3 \cdot \bar{u}$ ($M - R^2 = 0.6$, $p(F_{stat}) = 0$, DF = 91)

Note: bold face suggests some causes for high IE in the storm; last line in this table shows the multi-linear model resulted from stepwise variable selection followed by least squares linear regression.

[a] In this event there were 60 TF-gauges in the fixed subplot; it will be discussed again in 'Spatial variability of TF in the fixed subplot: observation with 60 TF-gauges' section.

53 mm and the coefficient of variation among the six raingauges <10%, by stepwise regression followed by least squares linear fit of standardized IE to the selected standardized variables (Sokal and Rohlf, 1995; Clarke, 1994). As implied in this standardized multi-linear empirical model, the rainfall intensity selected parameters, specially $IMAX_P$, are suggested to be negatively associated with IE, i.e., they tend to decrease IE; on the other hand, the meteorological condition during rain selected parameters, mean vapor pressure deficit and wind speed, that influence evaporation during rainfall, were suggested to be positively associated with IE. As reviewed by Lundberg et al. (1997), some studies have found large IE for high intense storms, in the present study site, however, such storms might be exceptional. In general, the above analysis suggests that long duration and low intensity events have higher IE than events of short duration and high intensity, in conformity with the review by Crockford and Richardson (2000). These trends that suggest low total IE during rainfall for both the short duration high intense storms that occurs in the afternoon when air is dry and windy, and during the long duration and low intensity storms that occurs in the morning under wet air and often calm wind, implies that water storage capacity, i.e., evaporation after rainfall ceases, is the governing factor in inter-storms or long-term IE quantities in the present site.

Noticeable variation among rainfall partitioned into TF, SF and IE in the fixed subplot were also suggested at yearly time scales (Table 7). Using SF data collected in Year 1, Manfroi et al. (2004) analyzed in more detail accumulated SF generation by the sampled trees; results for Year 2 and Year 3 were similar in that understory trees (DBH < 10 cm) were found to yield approximately 77% of the yearly accumulated SF in the fixed subplot and SF volume yield by individual trees was weakly associated with several simple to measure tree parameters. None of the measured tree parameters showed much better correlation with SF than the DBH of the trees. As shown in Table 7, however, lower SF, in spite of greater rainfall and slightly more frequent number of storms with $P > 20$ mm (Table 4), were observed in Year 2 and Year 3. Because SF usually increases with rainfall and maximizes after 20 mm of rainfall (Manfroi et al., 2004), the lower SF in these latter years might have resulted from deterioration of the stemflow collars or differences in the factors that affect SF among the years. In fact, some trees developed a callus bellow the collars, other might simple have grown in girth, compressing the collar outside and decreasing the aperture of the collar's outlet to the conducting hose, leaks were also more often found in the latter years. Multivariate analysis (principal components) and graphical analysis of SF in storms with $P > 20$ mm (not shown), suggested SF in the fixed subplot and for some individual trees to be decreased if storms had high mean intensity ($\overline{I_P}$) or high intensity spikes ($IMAX_P$). As other investigations of SF yield suggest, overflow of the collars in the more intense events, specially those with high intensity peaks, or branch flow could have been pronounced in the latter 2-years diverting potential SF to TF (Crockford and Richardson, 1987, 1990b, 2000; Herwitz, 1987). Nevertheless, the amount of rainfall partitioned into SF in the fixed subplot was relatively small in the 3 years, with annual mean of 76.1 mm/year or 3% of the mean annual P. As a result, the inter-yearly variation on IE is mostly attributable to differences in mean catches by the 20 fixed TF-gauges. This inter-annual variation could in part have been due to changes in the forest in the fixed subplot, differences in IE amounts during rainfall and variation in the accuracy of the true mean TF as determined with only 20 TF-gauges. As showed in Table 5, storms in Year 1 appeared of a lower intensity and associated with higher vapor pressure deficit. Such differences in storm characteristics could have affected both evaporation during rainfall and the accuracy of mean TF determined with 20 TF-gauges. Finally, as shown in Table 7, mean annual IE over these 3-years in the fixed subplot was 295 mm/year or 12% of the mean annual rainfall.

Spatial variability of TF in the fixed subplot: observation with 60 TF-gauges

In the 6-month period in Year 3 when TF in the fixed subplot was measured with the 20 fixed TF-gauges along with another 40 relocation TF-gauges, measurements were carried out 51 times for a total rainfall of 1150.1 mm. The total arithmetic mean TF caught by all 60 TF-gauges was 87.1(±20.2)% in the 6 months. If the 60 TF-gauges are separated into groups of 20 gauges, equally spread in the fixed subplot, however, the fixed TF-gauges (T1—T20) showed a total arithmetic mean TF of 87.8(±14.2)%, whereas this value was 89.0(±29.7)% for TF-gauges T21—T40 and 84.7(±13.3)% for TF-gauges T41—T60. Thus, the fixed TF-gauges caught the TF amounts closest to the mean of all 60 TF-gauges. The higher TF and variation in catches for TF-gauges T21—T40 was almost entirely due to the TF-gauge T26; excluding this TF-gauge the arithmetic mean of the remaining 19 TF-gauges decreased to 84.1(±21.3)%. Exclusion of such TF-gauges with high catches is, however, unjustifiable for reasons such as observational error or underestimation of rainfall. In the 6-month period, the TF catch of T26 was 180% of the total rainfall and that of a nearby TF-gauge, T27, was 134%. Overall, 10 TF-gauges

Table 7 Yearly accumulated TF, SF and IE observed in the fixed subplot

	P (mm)	TF (n = 20)		SF		IE	
		mm	% (SD)	mm	%	mm	%
Year 1	2292.0	1871.4	81.6 ± (17)	80.1	3.5	340.5	14.9
Year 2	2439.0	2134.1	87.5 ± (19)	68.3	2.8	236.6	9.7
Year 3	2668.0	2281.1	85.5 ± (12)	80.0	3.0	306.9	11.5
Average	2466.3	2095.5	85.0 ± (15)	76.1	3.1	294.7	12.0

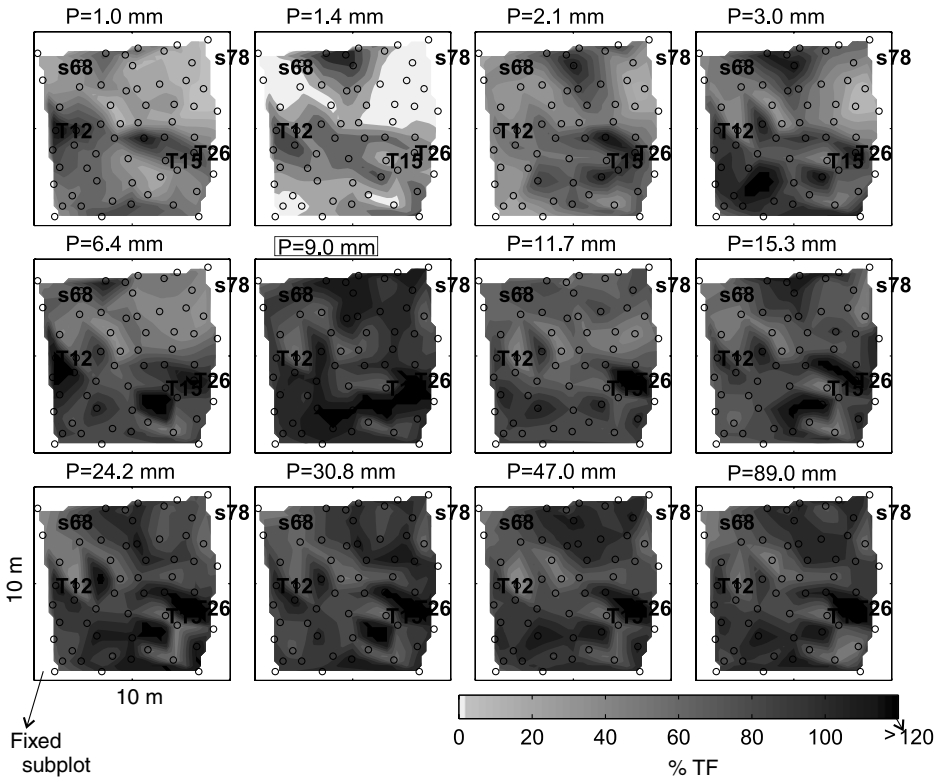

Figure 7 Contour plots of the triangular interpolated TF catches by the 60 TF-gauges in each of 12 storms of increasing depth (noted above the panel, e.g., P = 9.0 mm), in the fixed subplot. The circles marks the positions of the TF-gauges in the fixed subplot; positions of the two largest trees inside the fixed subplot (s78 and s68) and TF-gauges T12, T15 and T26 referred to in the text are also noted.

caught TF greater than rainfall in the 6 months, and 33 TF-gauges caught TF > 85%.

Fig. 7 shows contour plots of the spatial triangularly interpolated TF catches of the 60 individual TF-gauges in 12 storms of increasing depth using these TF-gauges x and y coordinates in the fixed subplot. In the 12 storms, the individual gauges catches varied between 0% and 235%; however, consistent occurring dripping zones, TF > 120%, occurred only near gauge T26. For 8 of the 12 storms shown, TF near gauge T26 was >180%. The TF-gauges near T26 were under the crown of an emergent tree with trunk outside the fixed subplot and with a broad and flat crown (indicated in Fig. 2); thus, horizontal rainwater movement created by the crown of this large tree have likely caused the intense dripping zones in this location in the fixed subplot with consequent TF decrease elsewhere under its about 200 m^2 crown area. On the other hand, TF-gauges with consistent low catches in all these 12 storms was only T15 which was under the crown of a high SF yielder understory tree (s22). The contour plot for the nighttime storm marked with P = 9.0 mm in Fig. 7, perhaps indicates areas in the fixed subplot where TF can be potentially high, which corresponds well to the less densely covered parts of the fixed subplot. Information on the climate conditions during this event was noted in Table 6, 'Partitioning of rainfall in the fixed subplot at the storm and yearly time scales' section, where the maximum rainfall caught among the six raingauges was used or 9.5 mm instead of mean catches by the 4 CPFB raingauges or 9 mm used here in Fig. 7. Assuming reference rainfall to be 9 mm, the mean TF caught by the 60 TF-gauges was 101% and there was a 2.4% SF in this storm, which means a negative IE of 3.4%. On the other hand, as it was shown in Table 6, assuming the maximum P catch among the six raingauges or 9.5 mm and the mean TF caught by the 20 fixed TF-gauges the calculated IE was −0.1%; finally, using the mean TF caught by the 60 TF-gauges in this storm and the 9.5 mm rainfall a 1% positive IE value results. This latter IE value is more reasonable, but still quite low for an event that occurred 18 h ahead of the previous one on a dry canopy; thus, underestimation of P, fog or mist deposition might have been involved. Other features worth noticing in Fig. 7, is that in storms with P < 3 mm, TF-gauges near trees s78 and s68, the two largest trees in the fixed subplot, tended to catch zero or small TF amounts, due to the dense canopy cover around these trees. In fact, in storms with P < 5 mm, variogram analysis suggested spatial correlation among the catches by the 60 individual TF-gauges, perhaps explainable by the low catch of TF-gauges close to the large trees, mainly near tree s78, in contrast to the high catches by TF-gauges near gaps (e.g., near T12). In storms with P > 5 mm, however, the variograms suggested a pure nugget effect or weak spatial correlation. In addition, somewhat persistent storm-to-storm TF spatial pattern in the fixed subplot for storms with P > 5 mm may be inferred from Fig. 7.

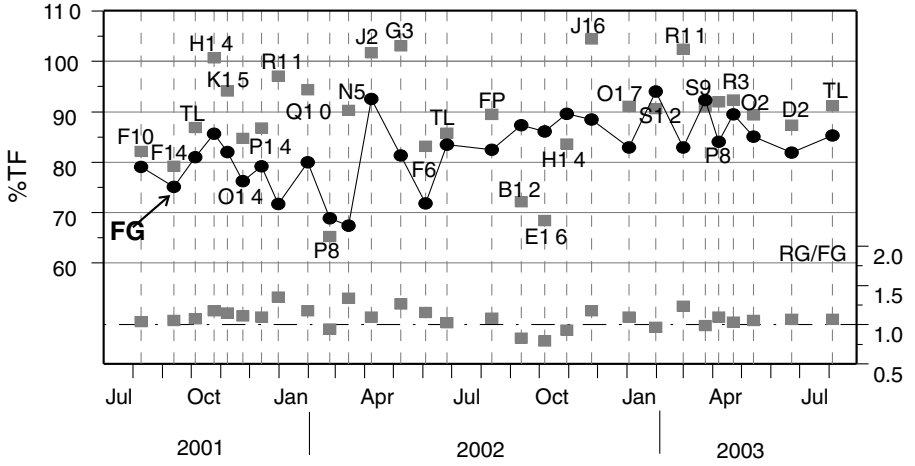

Figure 8 Short-term TF measured with the 20 relocation TF-gauges in the first 2-years in relocation positions. Showed are the arithmetic mean of the total TF, as a% of total rainfall, caught by the 20 relocation TF-gauges (RG) in the short-term TF measurements in Year 1 and 2 or relocation period, and that caught by the 20 fixed TF-gauges (FG) in the fixed subplot in the same short-term periods. The RG/FG ratio are also shown in the bellow part of the graph.

Spatial variability of TF in the 4-ha plot

Relocation versus fixed TF-gauges, and measurements with 100 TF-gauges

As shown in Fig. 8, the arithmetic mean TF caught by the 20 relocation TF-gauges (RG) in the subplots and transect line to where they were migrated in the first 2-years of this study, was almost always greater than that caught by the 20 fixed TF-gauges (FG) in the fixed subplot in the same period. Over the 2-years this was also true, while the arithmetic mean of the accumulated TF caught by the 20 RG migrated to different positions in the 4-ha plot was 90.5(±6.5)%, that of the 20 FG in the fixed subplot in the same 2-years was 84.2(±17)%. Considering this two years study separated, in Year 1 the RG mean catches was 92.4% and in Year 2 it was 88.6%; the high TF amounts caught by the RG in Year 1 may in part be related to the smaller basal area of subplots sampled in this year that was in mean 35.7 m^2/ha against 50 m^2/ha in the subplots sampled in Year 2. As discussed in previous sections, in the fixed subplot, the arithmetic mean catches by the FG, although lower, showed an opposite pattern with less TF in Year 1 (Table 7). Comparing mean TF caught by the RG and FG in 110 storms, taken from the single storms measurements data set, occurred in the first 2-years, also mean TF caught by the RG was more often higher than that caught by the FG in the fixed subplot (Fig. 9); particularly in storms of small size. This could also in part be explained by large interception or water holding capacity in the fixed subplot; as shown is Fig. 10, TF is negatively associated with a given subplot basal area, specially in storms of small size (<5 mm), and in the fixed subplot the basal area was the largest. Also, the variation in the RG by FG mean catches ratio (RG/FG) in these 110 storms were not patterned by rainfall intensity or during rainfall meteorological factors in a RG/FG to P graph. The three times repeated measurements, lagged by about a year, in the 60 m transect line (TL) starting in the border of the forest clearing about 15 m West of the crane's center and entering perpendicularly into the forest with the RG placed always at same points and 3 m apart, yielded similar ratios with the mean catches by the FG in the fixed subplot, or RG/FG (Fig. 8), and an overall arithmetic mean TF of 88.4% of the associated rainfall. In this transect, TF close to rainfall in the crane base (100%) were caught by three TF-gauges nearest the forest clearing, and TF < 60% by 3 TF-gauges located under stemless palms and the emergent tree apparently responsible for the dripping zones near TF-gauge T26 in the fixed subplot (see Fig. 2 and 'Spatial variability of TF in the fixed subplot: observation with 60 TF-gauges' section).

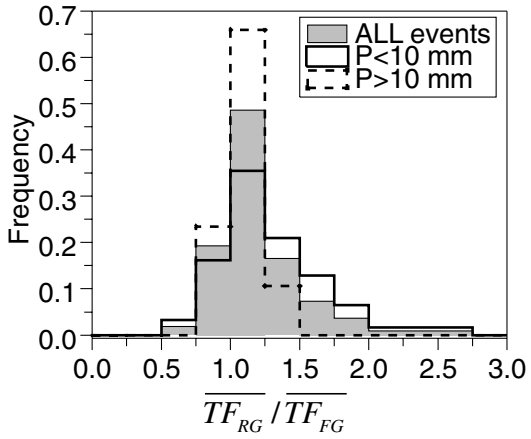

Figure 9 Comparison of relocation TF-gauges' mean catches with fixed TF-gauges mean catches in 110 single storms occurred in Year 1 and 2 or the 2-years relocation period. Showed are frequency histograms of the ratio of mean catches by the 20 relocation TF-gauges ($\overline{TF_{RG}}$) in a given position in the 4-ha plot by mean catches of the 20 fixed TF-gauges ($\overline{TF_{FG}}$) in the fixed subplot in each of the 110 single storms.

In the parallel TF measurements in five subplots in the latter 3-months of this study using 100 TF-gauges, i.e., the 20 fixed TF-gauges in the fixed subplot and other 20 TF-gauges per each of the relocation subplots (RP): H14, K15, D2 and J2; yielded a 3-months arithmetic mean accumulated catches by the 100 TF-gauges of

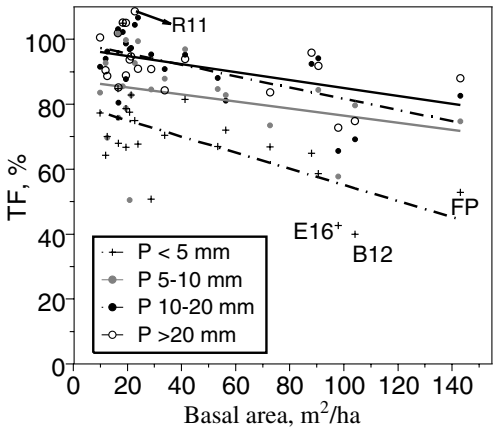

Figure 10 Relationship of mean TF observed in storms of four depth classes in the relocation subplots and fixed subplot (FP) with these subplots total basal area.

89.2(±21.1)%. Clear evidence that significant differences in rainfall received between subplots H14&K15 and subplots D2&J2, 120 m apart, affected the TF in these subplots were not found. In Table 8, mean TF per individual subplots in the 3-months and their corresponding value in the first 2-years relocation period as well as results for subplots R11 and P8 where measurements were done 2 times during the relocation period, are compared with the associated mean TF in the fixed subplot. As suggested from the last column in this table, on average in these six subplots with repeated measurements, TF was higher than concurrent measurements in the fixed subplot (RP/FP > 1). Comparing all data available for a same relocation subplot with the corresponding values in the fixed subplot in the same periods, also higher TF favored all relocation subplots (RP/FP > 1.02, penultimate line in Table 8). In addition, the resulting RP/FP ratio, calculated using all measurements, was negative associated with basal area in these four relocation subplots ($r_{Pearson}$ = −0.56). Therefore, somewhat high TF in long time scales are sensible in subplots like J2 where only small understory trees exist (TAGB = 1.3 t), but not >100% or greater than accumulated rainfall in the period as it resulted for both this subplot and subplot R11 (Table 8).

Explanation for the consistently greater than rainfall TF, and consequently negative IE, in repeated observations in subplots R11 and J2 are deferred to the next section. The noticeable TF and RP/FP ratio variation among periods of varying durations observed in subplots P8, H14, K15 and D2, shown in Table 8, also demands some comments. Such variations could have resulted from complex interactions between the canopy structure, rainfall and climate in each period that are unseen or smoothed out on more long time scales. It should be noticed from Fig. 8 that the highest TF values in the first 6 months in the first 2-years relocation period observed in the fixed subplot, and in relocation subplots was for the period the RG where in subplot H14. In this period, of 20 days, there were 22 storms or about 1.1 storms per day; the largest number of storms per day among all the short-term TF measurements in relocation positions. The second largest number of events per day during the relocation period was in subplot K15 and the third was in subplot J16. In all these periods, quite high TF were observed in

Table 8 Comparison of short-term mean TF observed in the relocation subplots (RP) where measurements where repeated a second time during the first 2-years relocation period or where measurements were done in the latter 3 months of the study, with mean TF observed in the fixed subplot (FP) in the same period

Period	Time	Position	P8	R11	H14	K15	D2	J2	Mean
Relocation period	1st, 14–40 days	RP	65.3	97.1	100.7	94.1	87.3	101.8	–
		FP	68.9	71.7	85.7	82.1	81.9	92.5	–
		RP/FP	0.95	1.35	1.18	1.15	1.07	1.10	1.12
		$P_{MAX} - \overline{P}$ (%)[a]	5.3	6.9	2.9	2.0	5.2	3.1	
	2nd, 14–23 days	RP	92	102.4	83.6	–	–	–	–
		FP	84.1	83	89.6	–	–	–	–
		RP/FP	1.09	1.23	0.93	–	–	–	1.07
		$P_{MAX} - \overline{P}$ (%)	8.5	5.0	2.4	–	–	–	–
Measured with 100 TF-gauges period, ≈3 months		RP	–	–	84.6	86.1	87.3	101.6	–
		FP	–	–	86.3	86.3	86.3	86.3	–
		RP/FP	–	–	0.98	1.0	1.01	1.18	1.04
		$P_{MAX} - \overline{P}$ (%)	–	–	2.2	2.2	2.2	2.2	–
All data, ≈1.5–4 months		RP	77.9	99.9	88.5	87.6	87.3	101.7	–
		FP	76.1	77.6	87.1	85.3	85.5	88.3	–
		RP/FP	1.02	1.29	1.02	1.03	1.02	1.15	1.09
		$P_{MAX} - \overline{P}$ (%)	4.6	5.9	2.0	2.6	3.5	1.8	–

[a] Difference between average rainfall ($\overline{P}$) and maximum rainfall (P_{MAX}) caught among the 4 CPFB raingauges.

relocation subplots (Fig. 8 and Table 8) but not always in the fixed subplot. On the other hand, during the measurements in subplot D2 in the relocation period there were only 15 storms in 40 days of observation; one of the lowest proportion of events per day. The two repeated measurements in subplot P8 (Table 8), in particular, suggests that TF can be significantly high in periods with many storms, even after considering uncertainties in rainfall, in these two periods accumulated rainfall was about 70 mm and size of storms were relatively identical and <10 mm, but in the first period there were 17 storms in 23 days and in the second period 12 storms in 14 days. In this latter period the arrangement of storms was more crowded, thus the canopy could only have dried out partially between storms; as a result, higher TF in both subplot P8 and in the fixed subplot were observed in the latter period than in the first period.

Dripping points: frequency and influence on subplots mean TF

By relocating 36 raingauges (∅ = 12.7 cm) every week, and sometimes after every storm, to randomly selected points in a grid with 505 marked positions along five transects crossing a 100 × 4 m or 0.04-ha plot of an Amazonian terra firma (non-flooded) tropical rainforest, Lloyd and Marques (1988) reported an arithmetic mean TF caught by the 36 relocated raingauges of 91% of the associated yearlong rainfall. Among 494 randomly observed points in the plot, in 29% the recorded TF catches were greater than rainfall recorded above canopy in the same period, and 46% of the total TF volume was observed at these points or dripping points. Also, while TF statistics between the five transects were not significant different, TF statistics derived for points grouped into five subgrid areas were significant different. Later observations by Ubarana (1996) at two nearby sites suggested similar results. Although in the present study we used a different TF-gauge (∅ = 20.6 cm) and different TF-gauges relocation system, similar results were obtained.

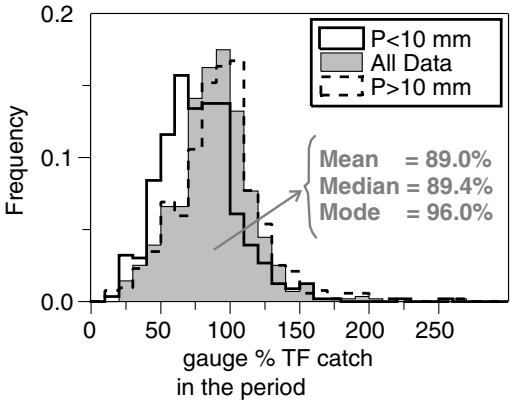

Figure 11 Distribution of TF observed in 560 unique points in the 4-ha plot. Showed are frequency histograms (bin = 10) of TF catches in 560 unique points located in 23 subplots and the transect line in the 4-ha plot. (*Note*: The histogram for 'All data' was computed with more than 10 measurements accumulated TF, in mean 15 storms, observed in a same unique point. Also, note that the mean, median and mode are shown for the 'All data' distribution; to calculate the mode data were rounded to the nearest integer first.)

As shown in Fig. 11, dripping points occurred frequently in the observed subplots even for storms with $P < 10$ mm; out of 560 points measured in the 23 subplots (0.23 ha) and the transect line in the 4-ha plot, TF catches were >100% in 31% of the points, and 45.1% of the total TF volume occurred at these points. Therefore, considerable horizontal movement of rainwater occurs in the canopy of lowland tropical rainforests which creates somewhat widely spaced drip points with a consequent TF reduction elsewhere (Shuttleworth, 1988). Enhanced branch flow in intense rain storms and the usually waxy long tipped leaves of tropical trees also might contribute to this concentrated TF areas or dripping zones (Ubarana, 1996; Herwitz, 1987).

As pointed out by Crockford and Richardson (2000), negative calculated IE suggests that net rainfall was over-estimated or rainfall was under-estimated. Due to the influence of dripping points in mean TF, in lowland tropical rainforests negative IE, calculated as the difference between P and TF + SF, are unexpected only in quite large plots. Also, because in some small plots of this forest vegetation is dense, or thick barked emergent trees are present and consequently mean TF tends to be reduced by significant water storage in foliage and trunks (Llorens and Gallart, 2000; Herwitz, 1985), or maybe rainwater diverted to other nearby plots through a broad and flat crown of some large trees, negative IE may result in some single storms but hardly for long periods of for example a month. This was exemplified in 'Spatial variability of TF in the fixed subplot: observation with 60 TF-gauges' section for the fixed subplot when due to the influence of some dripping points likely created by an outside tree with a broad flat crown the mean catches of 20 TF-gauges (T21—T40) in the fixed subplot was 3% higher in 6 months, and for many storms >6%, than the mean catches of TF-gauges placed more outside of the dripping area. For most of the storms, however, estimated IE with the mean catches by these TF-gauges would result positive in the fixed subplot. On the other hand, arguable, dripping points, often created by adjacent trees, have a different impact in mean TF observed in subplots with low biomass and likely small water holding capacity, as subplots R11 and J2 (Table 8). In fact, if two TF-gauges that caught 146.2% and 167.5% TF in subplot J2 are excluded, the recomputed mean TF in this subplot in the latter 3-months of this study changes from 101.7% (Table 8) to 95.5%; being this subplot DBH based estimated SF equal 2.5% a positive IE value of 3% is inferred.

Rainfall partition in the 4-ha plot

SF and TF scaled up to the 4-ha plot

Table 9 shows the linear regression equations relating yearly SVR, i.e., the total SF volume yield by an individual tree to total rainfall in the year or SF per millimeter of rainfall, to the DBH of 69 trees (for details, see Manfroi et al., 2004), and mean SF resulting of their application to the DBH > 1 cm of trees in the 22 relocation subplots and fixed subplot. On average 87.8 mm or 3.5% of the yearly rainfall was estimated to be partitioned into SF in the 22 subplots, i.e., the 4-ha plot SF is estimated to be only 12 mm higher than the amount observed in the fixed subplot with this method based on DBH data. Thus, the SF observation in the fixed subplot are representative of

Table 9 The SVR to DBH linear relationships derived from 69 trees measured for SF in each study year and mean SF calculated by applying such relationships to DBH > 1 cm data collected in the 22 relocation subplots and the fixed subplot (SD = standard deviation among subplots)

	SVR—DBH scaling equations, $n = 69$	$\overline{SF}$ (mm)	$\overline{SF}$ (%)	SD (%)
Year 1	SVR = $-12.6 + 133.5 \times \log 10(DBH)$, $R^2 = 0.49$	88.2	3.8	0.98
Year 2	SVR = $-13.3 + 119.5 \times \log 10(DBH)$, $R^2 = 0.49$	83.7	3.4	0.94
Year 3	SVR = $-9.0 + 114.3 \times \log 10(DBH)$, $R^2 = 0.45$	91.7	3.4	0.90
Average	SVR = $-11.6 + 122.4 \times \log 10(DBH)$, $R^2 = 0.48$	87.9	3.5	0.94

the 4-ha plot, specially for the purpose of IE calculation. Both the SF observed in the fixed subplot and estimated in the 4-ha plot in these years are, however, approximately twofold greater than those reported or assumed in many previous studies in tropical rainforests (Bruijnzeel, 1990; Crockford and Richardson, 2000), except for some studies that included trees in different growth stages and palms where SF amounts varying between 7% and 10% were observed (Frangi and Lugo, 1985; Jordan, 1978; Jordan and Heuveldop, 1981).

From the short-term TF measurements with the relocation TF-gauges in the first 2-years 29 least-squares linear regression equations relating TF to *P* were derived. The slope of these equations, i.e., TF per unit of rainfall, ranged from 0.75 to 1.15 with a mean of 0.94; *Y*-intercepts, however, were rational(<0) for 23 of these equations ranging from −0.1 to −1.3 mm, and a mean of −0.65 mm. Also, the coefficient of determination for such empirical models were high (0.97—0.99). These equations were then applied to storm's rainfall depth to fill up TF in the periods without observations in a given relocation position. Fig. 12 shows the short-term TF observed in the relocation positions and fixed subplot (also shown in Fig. 8) in the first 2-years, together with those estimated from the storms' rainfall depth in a given period without observation or in Year 3 with TF to *P* empirical static models. As shown, TF ratios between 85% and 95% were more frequently observed or estimated in these irregular periods. By combining the actual measurements of TF in the fixed subplot, short-term TF measured in relocation positions, and those estimated for the relocation positions with empirical linear TF to *P* equations, i.e., by summing up the rows in Fig. 12 over the 3-years study and averaging, a mean 3-years estimated TF of 88(±9.6)% was calculated; averaging over the yearly periods also a 88% TF resulted. This means a constant yearly fraction of rainfall partitioned into TF in the 4-ha plot level. The forest in the 4-ha plot, therefore, allowed approximately 3% greater TF than that actually observed in the fixed subplot in the 3 years (85%). Also, the estimated 4-ha plot mean TF of 88% with this method is similar to both the arithmetic mean of short-term TF observed in the 22 relocation subplots, or 88.5%, and the mean and median of the distribution of the relocation TF-gauges catches in 560 unique points in the 4-ha plot or 89% ('All Data', Fig. 11).

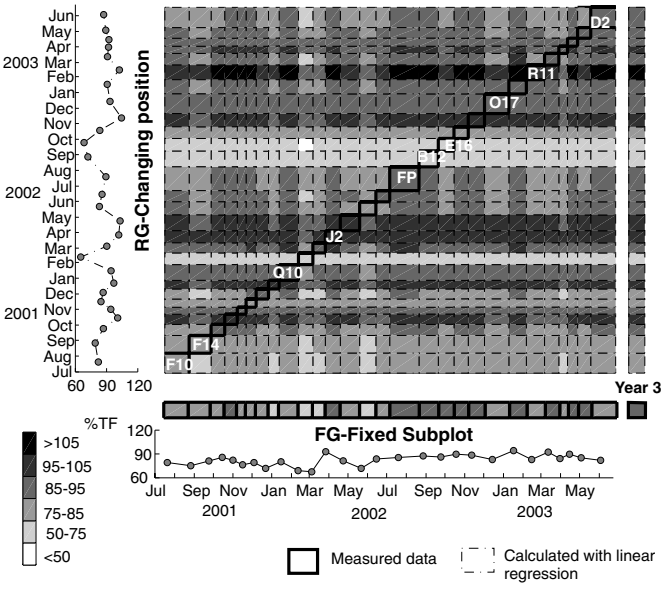

Figure 12 Illustration of time scaling up of TF, i.e., filling up of periods when TF measurements where not done in a given relocation position in the first two years or in the latter third year (Year 3). The observed mean TF in the relocation positions are shown in the left upper panel and diagonal of the gridded plot in the middle panel; those observed in the fixed subplot in the same period are shown in the bellow part of the graph.

Interception evaporation

The mean SF estimated for the 22 relocation subplots or 3.5% and the mean TF estimated in the 4-ha plot or 88% suggests a mean annual IE value of 8.5% in the 4-ha plot. Considering the long-term IE ''observed-estimated'' in the 22 relocation subplots individually their mean was also 8.5%; if the short-term TF observed in these subplots for 14 days to 5 months are used to compute these subplots IE the mean of the 22 subplots is 8.2%. Assuming that IE values calculated in the 22 subplots are a representative sample for the 4-ha plot and the storms occurred in the study period, the 95% lower and upper confidence intervals of the estimated mean annual IE from the 4-ha plot or 8.5% was computed from 1000 bootstrap samples' means. As a result the 4-ha plot mean annual IE was suggested to lie somewhere between 5% and 13%. Interpretation of the exponential relationship of estimated IE in the 22 relocation subplots and the fixed subplot with these subplots basal area (Fig. 13), also suggests that in the 4-ha plot, which mean basal area is 42 m^2/ha, long-term mean IE might be between 5% and 13%. As shown in Fig. 13, however, five subplots with estimated negative IE and two subplots (B12 and E16) with high IE of about 30% were calculated. As claimed in 'Dripping points: frequency and influence on subplots mean TF' section, the negative IE values have resulted from the influence of dripping points on mean TF observed in the five subplots, exemplified by subplots J2 and R11. As for the high IE values in subplots B12 and E16 they might be somewhat over-estimated due to under-estimation of SF. In subplot B12 there are four large stemless palm trees, not measured for SF, in the center of the plot and in subplot E16, seven of the 58 trees in this subplot are intermediate and main canopy layer trees, 20–70 cm in DBH, located clustered in the plot's center and with smooth bark. Also, in subplot F14 there are two large stemless palms. In fact, if three TF-gauges in the center of subplot B12 and under palms that caught TF between 25.6% and 40% of the 214 mm accumulated rainfall in the observation period in this subplot are excluded and the mean TF recalculated, this subplot estimated IE changes from 26% to 20% in the period. This latter value is inside the 95% confidence limits of the basal area to IE relationship showed in Fig. 13 and a sensible value for a subplot under an emergent large tree with thick bark, large amount of leaves and a crown projecting some 15 m from the main canopy layer. The effects of projecting crowns on IE, the high SF yielded by palm trees and also by intermediate trees with short branches and tall crowns for which less branch flow in intense rain might occurs have also been pointed out in previous studies (Lloyd and Marques, 1988; Schroth et al., 1999; Herwitz, 1987; Crockford and Richardson, 2000; Manfroi et al., 2004). Thus, although IE is probably high in subplots B12 and E16 a 5% higher SF than calculated using the trees's DBH in these subplots is sensible. Finally, based on this reasoning, if SF, including stemless palms, and TF had been observed for a long term in the 22 relocation subplots and assuming no drip influence on mean TF, then it is apparent that within the 4-ha area IE values between 3% and 25% in 10 × 10 m subplots could have resulted.

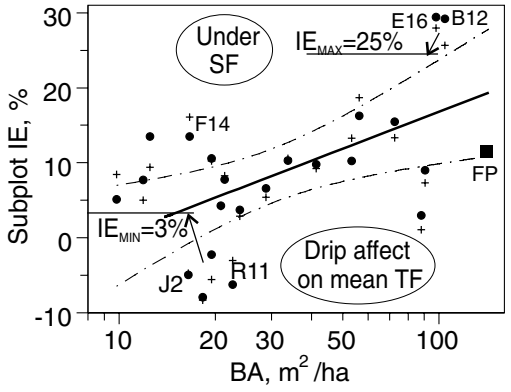

Figure 13 Relationship between the 3-years mean annual IE, estimated with the TF and SF scaling up methods, in 22 relocation subplots with these subplots basal area (●). The IE values calculated using only the 14 days to 5 months short-term mean TF observed in these subplots (+) and the 3-years IE value observed in the fixed subplot (■) are also shown.

Comparison of IE in the 4-ha plot with that observed in the fixed subplot and in previous studies

Table 10 shows the yearly rainfall partition observed in the fixed subplot, already shown in Table 7, and estimated in the 4-ha plot. The yearly 4-ha plot TF shown in Table 10 were calculated by applying the relocation positions empirical linear equations to the storms' depth in each study year while the SF values were already showed in Table 9. As a result, mean annual IE of 295 mm/year or 12% for the present site resulted from long-term static TF and SF observations in the fixed subplot, but that estimated in the 4-ha plot was 210 mm/year or 8.5%. In addition, annual IE in the fixed subplot was somewhat variable among the yearly studies, but that estimated in the 4-ha plot was constant. Given the large number of measurements carried out in the 3-years with the fixed TF-gauges in a same place in the fixed subplot the mean annual IE value derived for this subplot is arguably accurate. The inter-annual variability in IE, however, is difficult to discuss because of possible unmonitored changes in the forest canopy. Nevertheless, in Year 1, storms of low intensity were more numerous; given that in some moist tropical forest sites IE rates of about 50% of the annual rainfall have been attributed in part to the high storm frequency and low intensity rainfall regime in the site (Scatena, 1990), this might also have been the case in Year 1. Moreover, the mean annual IE we claim for the 4-ha plot might also be acceptable given that in the fixed subplot a large infrequent tree with thick bark, but small and not projecting crown, exists for which SF was only maximized after $P > 20$ mm. This large tree makes this subplot basal area to be 145 m^2/ha while the 4-ha plot mean basal area is only 42 m^2/ha. Interestingly, the difference between mean annual IE observed in the fixed subplot and that estimated in the 4-ha plot was 3.5% a figure equal the number of times the fixed subplot basal area exceeds the 4-ha plot mean or 3.4 times.

Fig. 14 shows a scatterplot of IE against rainfall reported in 37 previous case studies in moist tropical forests of the world that employed more than 12 fixed funnel type TF-gauges, any number of TF-gauges relocated periodically or

Table 10 Rainfall partitioned into TF, SF and IE in the fixed subplot and estimated in the 4-ha plot per yearly study

	P (mm)	Fixed subplot			4-ha plot		
		TF (%)	SF (%)	IE mm (%)	TF (%)	SF (%)	IE mm (%)
Year 1	2292.0	81.6	3.5	340.5(14.9)	87.5	3.8	199.4(8.7)
Year 2	2439.0	87.5	2.8	236.6(9.7)	88.0	3.4	209.8(8.6)
Year 3	2668.0	85.5	3.0	306.9(11.5)	88.3	3.4	221.4(8.3)
Average	2466.3	85.0	3.1	294.7(12)	87.9	3.5	210.2(8.5)

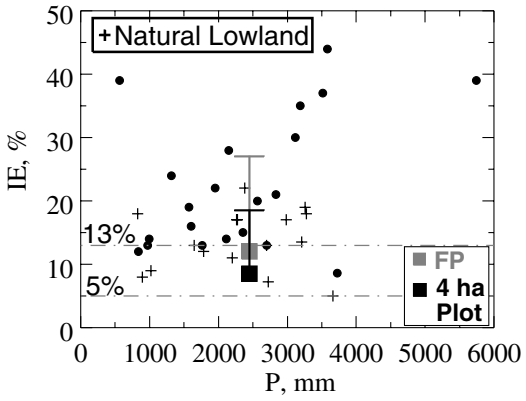

Figure 14 Relationship between mean annual IE and precipitation (*P*) observed in 37 previous case studies in tropical moist forests of the world and in the present study. Forests understood to be similar with the forest in the present site or natural lowland tropical forests are indicated with a cross (+), those not classified are indicated with filled circles. The *X*-axis or precipitation is the average yearly value if the study lasted for more than a year or the accumulated value if the study lasted for only a year or less than a year. (*Note*: Modified after Kuraji and Tanaka (2003).)

any number of troughs. The 4-ha plot estimated IE and that observed in the fixed subplot are also shown with an error - bar in the positive direction corresponding to the standard deviation of estimated TF over the 3 years in the relocation positions (10%) or the standard deviation among the accumulated fixed TF-gauges catches over the 3-years (15%). As shown, many studies reported IE between 10% and 20% of the associated rainfall and in all studies carried out in forests we understood to be quite similar to the forest in the 4-ha plot, or lowland tropical forest sites, IE < 20% were claimed, except for a study in Pasoh forest reserve, Peninsular Malaysia, where a 22% IE was reported (Manokaran, 1979). The 95% confidence limits we estimated for the 4-ha plot IE or 5—13% encompass only half of the previous studies' results in lowland tropical forests, but in the 4-ha area IE values from 3% to 25% are also possible in 10×10 m subplots. In Amazonian terra firma (non-flooded) forests IE values in the 5—13% range have been claimed both from observation and micrometeorological evaporation modeling (Ubarana, 1996; Lloyd and Marques, 1988; Lloyd et al., 1988; Jordan and Heuveldop, 1981; Shuttleworth, 1988). Observations carried out by Marin et al. (2000) in four ecosystems in western Amazonia lowlands suggested for three of the ecosystems long-term IE values between 12% and 13% but in a flood plain ecosystem with a relatively smaller gap fraction, a 17% value was estimated. In all of these four ecosystems, the SF yield of trees with DBH > 10 cm was <1.54%, with an average of 1.1%. If palms or a dense understory were present in the studied plots, which could be the case in the flood plain ecosystem where leaf area index was the highest, it is possible that SF could have been under-estimated in some of the study plots. In the study of Frangi and Lugo (1985), for instance, also in a flood plain ecosystem, though in subtropical Puerto Rico, TF measurements in a 2525-m^2 plot with 20 fixed TF-gauges resulted in a 81.6% TF that added to 2% SF would suggest a 17% IE value, but actual observations of SF of 26 trees including palms in a 100-m^2 subplot resulted in a SF value of 9.8% and consequently IE of 8.6%. Nevertheless, the 8.6% IE value reported in this latter study and those in the three of the ecosystems studied by Marin et al. (2000) of approximately 12.4% are inside the 95% confidence limit we estimated for the IE in the 4-ha plot. Also, in Ivory Coast, west Africa, Hutjes et al. (1990) reported a 9.2% IE value over 6 months in a primary lowland evergreen tropical forest.

The lack of consensus whether mean annual IE varies somewhat broadly in lowland tropical forests is more clear in studies conducted in southeast Asia. In peninsular Malaysia lowland tropical forests values between 13% and 22% were reported (Tani et al., 2003; Manokaran, 1979; Zulkifli, 1996) and in Borneo Island values between 8% and 20% (Sinun et al., 1992; Dykes, 1997; Burghouts et al., 1998; Asdak et al., 1998; Chappell et al., 2001). The 11% IE value claimed for a natural lowland tropical forest in central Kalimantan, Indonesian Borneo, by Asdak et al. (1998), although similar to the 12% IE we observed in the fixed subplot might be somewhat over-estimated given that only the SF of commercial wood or trees with DBH > 10 cm were observed resulting in a 1.4% SF. Thus, because our study suggested that trees with DBH < 10 cm may contribute with another 2% to the SF, a 9% IE could also have been possible in this case study if a dense understory existed. This latter figure is close to our 4-ha plot estimated mean annual IE and that obtained in northern Borneo at the Danum Valley Field Center by Chappell et al. (2001) or 8% (SF of 1% assumed).

Conclusions

The canopy of lowland evergreen tropical forests are highly variable in both the horizontal and vertical directions, making their interactions with rainfall and climate complex and localized. As a result, formidable spatial and temporal variations in net rainfall (SF + TF) inside these forests exist. In the 4-ha plot studied here spatial variation in basal area, location of large trees that sometimes have a projecting

broad crown, or high SF yielding trees and stemless palms were some of the causes of a −6% to 30% range of IE values derived in 23 small subplots within this 4-ha area. By considering dripping points influence on the mean TF in subplots with negative IE and under-estimation of SF in two subplots with about 30% IE values, still a range of IE values between 3% and 25% was thought sensible among the 23 subplots within the 4-ha area. This range encompasses all mean annual IE values claimed in previous studies in natural lowland tropical forests. Thus, to facilitate IE reviewers to separate effects of forest, rainfall, climate and methodological issues on mean annual IE or inter-storms IE variation, and to make inter-site comparisons, researchers should document well the forest site, the observed plot, rainfall and climate in the study period. Moreover, if the IE values derived will be used in water balance studies or for comparison with model's predictions that require representative spatial averages the size and location of the observed plot have to be thought carefully along with the observation design and the duration of the study.

Notwithstanding the high within subplots variation among catches of individual TF-gauges, we claimed for the 4-ha plot area a mean annual IE of 8.5% with 95% confidence limits between 5% and 13%, and small inter-annual variation (<1%). This mean annual IE value, and those observed in the fixed subplot scale (<15%), are surprisingly low for a forest with trees between 40 and 70 m height and large above ground biomass, perhaps one of the highest values among tropical moist forests, and also given the high frequency of storms in the present site. Based on our simple analysis of factors causing inter-storms IE variations or inter periods TF variations, we suggest that if in a yearlong period storms well separated from each other, i.e., long inter-arrival times, with long duration or low intensity and associated with dry windy atmosphere predominate the rainfall regime, then in such years IE values >15% from the 4-ha area are possible. The rainfall regime in the present site, however, has many storms in night time or in the morning under wet atmosphere, and the storms occurred in the noon under dry atmosphere were usually of short duration and high intensity.

Acknowledgements

This research was supported by the Core Research for Evolutional Science and Technology (CREST) fund of the Japan Science and Technology Corporation (JST). The first author is a scholarship student of the Japanese Ministry of Education, Culture, Sports, Science and Technology, to whom we express sincere gratitude. We also thank Lucy Chong and the staff of the Forest Research Center of Sarawak for their help and support to our research.

References

Asdak, C., Jarvis, P.G., Gardingen, P.v., Fraser, A., 1998. Rainfall interception loss in unlogged and logged forest areas of central Kalimantan, Indonesia. Journal of Hydrology 206, 237–244.

Bonell, M., Balek, J., 1993. Recent scientific developments and research needs in hydrological processes of the humid tropics. In: Bonell, M., Hufschmidt, M.M., Gladwell, J.S. (Eds.), Hydrology and Water Management in the Humid Tropics: Hydrological Research Issues and Strategies for Water Management. Cambridge University Press, Cambridge, pp. 167–260.

Bouten, W., Schaap, M.G., Aerts, J., Vermetten, A.W.M., 1996. Monitoring and modelling canopy water storage amounts in support of atmospheric deposition studies. Journal of Hydrology 181 (1–4), 305–321.

Brown, A.E., Zhang, L., McMahon, T.A., Western, A.W., Vertessy, R.A., 2005. A review of paired catchment studies for determining changes in water yield resulting from alterations in vegetation. Journal of Hydrology 310 (1–4), 28–61.

Bruijnzeel, L.A., 1990. Hydrology of Moist Tropical Forests and Effects of Conversion: A State of Knowledge Review. UNESCO, Paris, 224pp.

Burghouts, T.B.A., Straalen, N.M.V., Bruijnzeel, L.A., 1998. Spatial heterogeneity of element and litter turnover in a bornean rain forest. Journal of Tropical Ecology 14, 477–505.

Calder, I.R., 1993. Hydrologic effects of land-use change. In: Maidment, D.R. (Ed.), Handbook of Hydrology. McGraw-Hill, New York, pp. 13.1–13.50.

Calder, I.R., 2003. Assessing the water use of short vegetation and forests: development of the Hydrological Land Use Change (HYLUC) model. Water Resources Research 39 (11), 1318, WR002040.

Calder, I.R., 2004. EXLAIM (Exploratory, Climate, Land, Assessment, Impact, Management) GIS tool (University of Newcastle: accessed 20 January 2005). Available from: <http://www.cluwrr.ncl.ac.uk/index.html>; Internet.

Calder, I.R., Rosier, P.T.W., 1976. The design of large plastic-sheet net-rainfall gauges. Journal of Hydrology 30 (4), 403–405.

Calder, I.R., Wright, I.R., 1986. Gamma-ray attenuation studies of interception from Sitka Spruce: some evidence for an additional transport mechanism. Water Resources Research 22 (3), 409–417.

Chappell, N.A., Bidin, K., Tych, W., 2001. Modelling rainfall and canopy controls on net-precipitation beneath selectively-logged tropical forest. Plant Ecology 153, 215–229.

Chave, J., Condit, R., Lao, S., Caspersen, J.P., Foster, R.B., Hubbell, S.P., 2003. Spatial and temporal variation of biomass in a tropical forest: results from a large census plot in Panama. Journal of Ecology 91, 240–252.

Choudhury, B.J., DiGirolamo, N.E., 1998. A biophysical process-based estimate of global land surface evaporation using satellite and ancillary data i. Model description and comparison with observations. Journal of Hydrology 205 (3–4), 164–185.

Clarke, R.T., 1987. The interception process in tropical rain forest: a literature review and critique. Acta Amazonica 16/17, 225–238.

Clarke, R.T., 1994. Statistical Modeling in Hydrology. Wiley, Chichester.

Crockford, R.H., Johnson, M.E., 1983. Some errors in the measurement of precipitation, throughfall and stemflow and implications for estimation of interception. In: Hydrology and Water Resources Symposium, Hobart, Tasmania. Conference publication No. 86/13. Institute of Engineers, Australia, pp. 236–242.

Crockford, R.H., Richardson, D.P., 1987. Factors affecting the stemflow yield of a Dry Sclerophyll Eucalypt Forest, a *Pinus radiata* plantation and individual trees within these forests. Technical Memorandum 87/11. Division of Water Resources Research, CSIRO.

Crockford, R.H., Richardson, D.P., 1990a. Partitioning of rainfall in a eucalypt forest and pine plantation in southeastern Australia: I. Throughfall measurement in a eucalypt forest: effect of method and species composition. Hydrological Processes 4, 131–144.

Crockford, R.H., Richardson, D.P., 1990b. Partitioning of rainfall in a eucalypt forest and pine plantation in southeastern Australia. II. Stemflow and factors affecting stemflow in a dry sclerophyll

eucalypt forest and a *Pinus radiata* plantation. Hydrological Processes 4, 145–155.
Crockford, R.H., Richardson, D.P., 1990c. Partitioning of rainfall in a eucalypt forest and pine plantation in southeastern Australia. IV. The relationship of interception and canopy storage capacity, the interception of these forests, and the effect on interception of thinning the pine plantation. Hydrological Processes 4, 169–188.
Crockford, R.H., Richardson, D.P., 2000. Partitioning of rainfall into throughfall, stemflow and interception: effect of forest type, ground cover and climate. Hydrological Processes 14, 2903–2920.
Crockford, R.H., Richardson, D.P., Sageman, R., 1996. Chemistry of rainfall, throughfall and stemflow in a eucalypt forest and a pine plantation in south-eastern Australia. 1. Rainfall. Hydrological Processes 10, 1–11.
Dykes, A.P., 1997. Rainfall interception from a lowland tropical rainforest in Brunei. Journal of Hydrology 200, 260–279.
FAO, 1993. Food and agriculture organization. Forest resources assessment 1990-tropical countries. Technical report, FAO Forestry Paper 112.
Frangi, J.L., Lugo, A., 1985. Ecosystem dynamics of a subtropical floodplain forest. Ecological Monographs 55 (3), 351–369.
Habib, E., Krajewski, W.F., Kruger, A., 2001. Sampling errors of tipping-bucket rain gauge measurements. Journal of Hydrologic Engineering 6 (2), 159–166.
Herwitz, S.R., 1985. Interception storage capacities of tropical rain forest canopy trees. Journal of Hydrology 77, 237–252.
Herwitz, S.R., 1987. Raindrop impact and water flow on the vegetative surfaces of trees and the effect on stemflow and throughfall generation. Earth Surface Processes Landforms 12, 425–432.
Hölscher, D., Köhler, L., van Dijk, A.I.J.M., Bruijnzeel, L.A.S., 2004. The importance of epiphytes to total rainfall interception by a tropical montane rain forest in Costa Rica. Journal of Hydrology 292 (1–4), 308–322.
Horton, R.E., 1919. Rainfall interception. Monthly Weather Review 47, 603–623.
Hutjes, R.W.A., Wierda, A., Veen, A.W.L., 1990. Rainfall interception in the Tai forest, Ivory Coast: application of two simulation models to a humid tropical system. Journal of Hydrology 114, 259–276.
Jackson, I.J., 1971. Problems of throughfall and interception assessment under tropical forest. Journal of Hydrology 12 (3), 234–254.
Jordan, C.F., 1978. Stem flow and nutrient transfer in a tropical rainforest. Oikos 31, 257–263.
Jordan, C.F., Heuveldop, J., 1981. The water budget of an Amazonian rain forest. Acta Amazonica 11, 87–92.
Kimmins, J.P., 1973. Some statistical aspects of sampling throughfall precipitation in nutrient cycling studies in British Columbian coastal forests. Ecology 54, 1008–1019.
Kumagai, T., Kuraji, K., Noguchi, H., Tanaka, Y., Tanaka, K., Suziki, M., 2001. Vertical profiles of environmental factors within tropical rainforest, Lambir Hills National Park, Sarawak, Malaysia. Journal of Forest Research 6, 257–264.
Kumagai, T., Saitoh, T.M., Sato, Y., Morooka, T., Manfroi, O.J., Kuraji, K., Suzuki, M., 2004. Transpiration, canopy conductance and the decoupling coefficient of a lowland mixed dipterocarp forest in Sarawak, Borneo: dry spell effects. Journal of Hydrology 287 (1–4), 237–251.
Kumagai, T., Saitoh, T.M., Sato, Y., Takahashi, H., Manfroi, O.J., Morooka, T., Kuraji, K., Suzuki, M., Yasunari, T., Komatsu, H., 2005. Annual water balance and seasonality of evapotranspiration in a bornean tropical rainforest. Agricultural and Forest Meteorology 128 (1–2), 81–92.
Kume, T., Kuraji, K., Yoshifuji, N., Morooka, T., Sawano, S., Chong, L., Suzuki, M., 2005. Estimation of canopy drying time after rainfall using sap flow measurements in an emergent tree in a lowland mixed-dipterocarp forest in Sarawak, Malaysia. Hydrological Processes 20, 565–578.
Kuraji, K., Tanaka, N., 2003. Rainfall interception studies in the tropical forests. Journal of Japanese Forestry Society 85 (1), 18–28 (in Japanese with English abstract).
Kuraji, K., Tanaka, Y., Kumagai, T., Suzuki, M., 2001. Long-term monitoring of the physical environment in and above the canopy and underground in Lambir Hills National Park. In: Ichioka, T., Nakashizuka, T., Chong, L. (Eds.), Canopy Processes and Ecological Roles of Tropical Rain Forest. Forest Department Sarawak and Japan Science and Technology Corporation, Miri, Sarawak, Malaysia, pp. 72–77.
Lee, H.S., Davies, S.J., Lafrankie, J.V., Tan, S., Yamakura, T., Itoh, A., Ohkubo, T., Ashton, P.S., 2002. Floristic and structural diversity of mixed dipterocarp forest in Lambir Hills National Park, Sarawak, Malaysia. Journal of Tropical Forest Science 14, 379–400.
Leopoldo, P.R., Franken, W.K., Villa Nova, N.A., 1995. Real evapotranspiration and transpiration through a tropical rain forest in central Amazonia as estimated by the water balance method. Forest Ecology and Management 73 (1–3), 185–195.
Llorens, P., Gallart, F., 2000. A simplified method for forest water storage capacity measurement. Journal of Hydrology 240 (1–2), 131–144.
Llorens, P., Poch, R., Latron, J., Gallart, F., 1997. Rainfall interception by a *Pinus sylvestris* forest patch overgrown in a Mediterranean mountainous abandoned area i. Monitoring design and results down to the event scale. Journal of Hydrology 199 (3–4), 331–345.
Lloyd, C.R., 1990. The temporal distribution of Amazonian rainfall and its implications for forest interception. Quarterly Journal of the Royal Meteorological Society 116 (496), 1487–1494.
Lloyd, C.R., Marques, F.A.D.O., 1988. Spatial variability of throughfall and stemflow measurements in Amazonian rainforest. Agricultural and Forest Meteorology 42, 63–74.
Lloyd, C.R., Gash, J.H.C., Shuttleworth, W.J., 1988. The measurement and modeling of rainfall interception by Amazonian rainforest. Agricultural and Forest Meteorology 43, 277–294.
Lundberg, A., Eriksson, M., Halldin, S., Kellner, E., Seibert, L., 1997. Interception evaporation: review of existing and new measurement techniques. Journal of Atmospheric Oceanic Technology 14, 130–142.
Malhi, Y., Wright, J., 2004. Spatial patterns and recent trends in the climate of tropical rainforest regions. Philosophical Transactions of the Royal Society of London Series B 359, 311–329.
Manfroi, O.J., Kuraji, K., Tanaka, N., Suzuki, M., Nakagawa, M., Nakashizuka, T., Chong, L., 2004. The stemfow of trees in a Bornean lowland tropical forest. Hydrological Processes 18, 2455–2474.
Manokaran, M., 1979. Stemflow, throughfall and rainfall interception in a lowland tropical rain forest in Peninsular Malaysia. Malaysian Forester 42, 174–200.
Marin, C.T., Bouten, W., Sevink, J., 2000. Gross rainfall and its partitioning into throughfall, stemflow and evaporation of intercepted water in four forest ecosystems in western Amazonia. Journal of Hydrology 237 (1–2), 40–57.
Mizutani, K., Ikeda, T., 1994. Evaporation of intercepted rainfall from a *Castanopsis cuspidata* Schottky forest using various micrometeorological methods. In: International Symposium on Forest Hydrology. IUFRO, Tokyo, Japan, pp. 69–76.
NIMA, 1996. Digital terrain elevation data level 0. Technical report, National Imagery and Mapping Agency.
Noguchi, S., Nik, A.R., Tani, M., 2003. Rainfall characteristics of tropical rainforest at Pasoh forest reserve, Negeri Sembilan, Peninsular Malaysia. In: Okuda, T., Manokaran, M., Matsumoto, Y., Niiyama, K., Thomas, S., Ashton, P.S. (Eds.), Pasoh: Ecology of a Lowland Rain Forest in Southeast Asia. Springer, Tokyo, pp. 51–58.

Oki, T., Musiake, K., 1994. Seasonal change of the diurnal cycle of precipitation over Japan and Malaysia. Journal of Applied Meteorology 33, 1445–1463.

Rutter, A.J., 1963. Studies in the water relations of *Pinus sylvestris* in plantation conditions. Measurements of rainfall and interception. Journal of Ecology 51, 191–203.

Scatena, F.N., 1990. Watershed scale rainfall interception on two forested watersheds in the Luquillo mountains of Puerto Rico. Journal of Hydrology 113, 89–102.

Schroth, G., da Silva, L.F., Wolf, M.A., Teixeira, W.G., Zech, W., 1999. Distribution of throughfall and stemflow in multi-strata agroforestry, perennial monoculture, fallow and primary forest in central Amazonia, Brazil. Hydrological Processes 13 (10), 1423–1436.

Shuttleworth, W.J., 1988. Evaporation from Amazonian rainforest. Philosophical Transactions of the Royal Society of London Series B 233, 321–346.

Shuttleworth, W.J., 1989. Micrometeorology of temperate and tropical forest. Philosophical Transactions of the Royal Society of London Series B 324, 299–334.

Sinun, W., Meng, W.W., Douglas, I., Spencer, T., 1992. Throughfall, stemflow, overland flow and throughflow in the Ulu Segama rain forest, Sabah, Malaysia. Philosophical Transactions of the Royal Society of London Series B 335, 389–395.

Sokal, R., Rohlf, F., 1995. Biometry: The Principles and Practice of Statistics in Biological Research, third ed. W.H. Freeman, New York.

Tani, M., Nik, A.R., Yasuda, Y., Noguchi, S., Shamsuddin, S., Sahat, M., Takanashi, S., 2003. Long-term estimation of evapotranspiration from a tropical rain forest in Peninsular Malaysia. In: Franks, S.W., Böschl, G., Kumagai, M., Musiake, K., Rosbjerg, D. (Eds.), Water Resources Systems Water Availability and Global Change, vol. 280. IAHS, Sapporo, Japan, pp. 267–274.

Ubarana, V.N., 1996. Observations and modelling of rainfall interception at two experimental sites in Amazônia. In: Victoria, R.L., Gash, J.H.C., Nobre, C.A., Roberts, C.A. (Eds.), Amazonian Deforestation and Climate. Wiley, New York, pp. 151–162.

Whitmore, T.C., 1998. An Introduction to Tropical Rainforests, second ed. Oxford University Press, New York, 224pp.

Wilm, H.G., 1943. Determining net rainfall under a conifer forest. Journal of Agricultural Research 67, 501–513.

Zulkifli, Y., 1996. Nutrient cycling in secondary rain forest catchments of Peninsular Malaysia. Thesis, University of Manchester, 380pp.